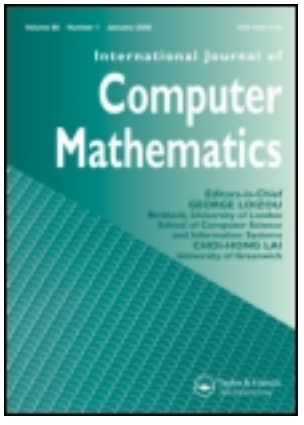

International Journal of Computer Mathematics
Publication details, including instructions for authors and subscription information:
http://www.tandfonline.com/loi/gcom20

Adaptive synchronization of complex networks

P. De Lellis [a], M. Di Bernardo [a], F. Sorrentino [a] & A. Tierno [a]
[a] Department of Computer and Systems Engineering, Università di Napoli Federico II, Napoli, Italy
Version of record first published: 07 Aug 2008.

To cite this article: P. De Lellis , M. Di Bernardo , F. Sorrentino & A. Tierno (2008): Adaptive synchronization of complex networks, International Journal of Computer Mathematics, 85:8, 1189-1218

To link to this article: http://dx.doi.org/10.1080/00207160701704580

International Journal of Computer Mathematics
Vol. 85, No. 8, August 2008, 1189–1218

Adaptive synchronization of complex networks

P. De Lellis*, M. Di Bernardo, F. Sorrentino and A. Tierno

Department of Computer and Systems Engineering, Università di Napoli Federico II, Napoli, Italy

(*Received 25 July 2007; revised version received 18 September 2007; accepted 20 September 2007*)

The aim of this paper is to propose and validate numerically a set of novel adaptive strategies for synchronization and consensus of complex networks of dynamical systems. We present both centralized and decentralized strategies where the adaptation law is based on, respectively, global and local information at the network nodes. All the proposed adaptive techniques are then validated using computer simulations on ensembles of two types of oscillators: Kuramoto and Rössler. We show that, in both cases, synchronization can be achieved with the adaptive gains reaching asymptotically finite steady-state values.

Keywords: synchronization; complex networks; adaptive control; consensus; Kuramoto oscillators

AMS Subject Classification: 93C40; 90B10; 34C15; 34C28

1. Introduction

Networked systems abound in nature and in applied science. Networks of dynamical systems have been recently proposed as models in many diverse fields of applications (see, for instance, [1,9] and references therein).

Recently, particular attention has been focused on the problem of making a network of dynamical systems synchronize on a common evolution. Typically, the network consists of N identical nonlinear dynamical systems coupled through the edges of the network itself [1,9]. Each uncoupled system is described by a nonlinear set of ordinary differential equations (ODEs) of the form $\dot{x} = f(x)$, where $x \in R^n$ is the state vector and $f : R^n \mapsto R^n$ is a sufficiently smooth nonlinear vector field describing the system dynamics. Because of the coupling with the neighbouring nodes in the network, the dynamics of each oscillator is affected by a nonlinear input representing the interaction of all neighbouring nodes with the oscillator itself. Hence, the equations of motion for the generic ith system in the network become

$$\frac{\mathrm{d}x_i}{\mathrm{d}t} = f(x_i) - \sigma \sum_{j=1}^{N} \mathcal{L}_{ij} h(x_j), \quad i = 1, 2, \ldots, N, \tag{1}$$

where x_i represents the state vector of the ith oscillator, σ the overall strength of the coupling, $h(x) : R^n \mapsto R^n$ the output function through which the systems in the network are coupled, and

*Corresponding author. Email: pietro.delellis@unina.it

ISSN 0020-7160 print/ISSN 1029-0265 online

DOI: 10.1080/00207160701704580
http://www.informaworld.com

$\mathcal{L}_{ij}$ the elements of the Laplacian matrix $\mathcal{L}$ describing the network topology. In particular, $\mathcal{L}$ is such that its entries, $\mathcal{L}_{ij}$, are zero if node i is not connected to node $j \neq i$, and are negative if node i is connected to node j, with $\mid \mathcal{L}_{ij} \mid$ giving a measure of the strength of the interaction.

Now, the problem is to find σ so that all the systems in the network synchronize on the same evolution, say $x_s(t)$. Specifically, one wants to find an appropriate value of σ such that

$$\lim_{t\to\infty} (x_i(t) - x_j(t)) = 0$$

for all pairs $(i,\ j)$ of nodes such that $i \neq j$. An approach based on the so-called master stability function (MSF) has been established to evaluate the range of σ for which synchronization is locally attained [1]. Basically, it has been shown that the width of the range of values of the coupling gain associated with the transversal stability of the synchronization manifold is related to the ratio between the largest and the smallest non-zero eigenvalue of the network Laplacian $\mathcal{L}$. Such a ratio is often referred to as the network eigenratio. The MSF gives an indication of the network synchronizability, in terms of the values of σ for which synchronization can be achieved.

In general, the coupling gain is chosen to be identical for all edges in the network and constant in time. Many real-world networks are characterized instead by evolving, adapting coupling gains which vary in time according to different environmental conditions. For example, we can mention wireless networks of sensors that gather and communicate data to a central base station [8]. Adaptation is also necessary to control networks of robots when the conditions change unexpectedly (i.e. a robot loses a sensor) [12]. Moreover, examples of adaptive networks could be found in biology. Social insect colonies, for instance, have many of the properties of adaptive networks [3].

The aim of this paper is to propose and explore a set of novel adaptive synchronization strategies where the coupling gain σ becomes a function of time, i.e. $\sigma = \sigma(t)$ in the simplest case. We explore two main types of adaptation mechanisms: (1) a global adaptation strategy where $\sigma = \sigma(t)$ is the same for all nodes and edges in the networks; (2) a local, decentralized, adaptation strategy where each node or edge is associated with an adaptive coupling gain (e.g. the gain $\sigma_{ij}(t)$ will be associated with the edge between the nodes i and j). We will show that under appropriate conditions, both strategies ensure the asymptotic synchronization of all the network systems, with the adaptive gains tending to constant asymptotic values by means of our proposed strategies. It is worth mentioning here that, as shown in the paper, some interesting conclusions can be drawn on the nature of the network under investigation by looking at the limits of the adaptive gain evolutions as well as their magnitudes and distribution among the nodes and edges of the network. Also, interesting effects can be observed, which are related to the topological features of the network itself.

The idea of using time-varying gains to synchronize networks of coupled dynamical systems has been discussed little in the vast existing literature on synchronization of complex networks. In their recent work, Kurths and Zhou [6] introduce a scheme of decentralized weight adaptation that leads to global synchronization of a network of Rössler chaotic systems. Other researchers have proposed an adaptive controller of the dynamics of all nodes to achieve synchronization in the presence of uncertain parameters [2,7].

The rest of the paper is outlined as follows. In Section 2, we describe the novel adaptive approaches studied in the paper. Then in Section 3, we validate the proposed strategies on a network of identical Kuramoto oscillators. The case of Rössler oscillators coupled on the x-variable is considered next in Section 4, whereas in Section 5, coupling on all the three state variables is investigated. An analysis of the factors that influence the convergence speed is presented in Section 6. Finally, the performances of the proposed schemes are further tested in Section 7, where the adaptive synchronization of non-identical oscillators is analyzed numerically. Conclusions are finally drawn in Section 8.

2. An adaptive approach

As a first simple way of introducing an adaptive mechanism in the synchronization of complex networks, we propose making the gain σ in Equation (1) a function of time and then assigning a continuous time differential adaptive law for σ. In particular, we have

$$\frac{\mathrm{d}x_i}{\mathrm{d}t} = f(x_i) - \sigma(t)\sum_{j=1}^{N}\mathcal{L}_{ij}h(x_j), \quad i = 1, 2, \ldots, N, \tag{2}$$

with $\sigma(t)$ given by a differential equation of the form

$$\dot{\sigma}(t) = \phi(x_1, x_2, \ldots, x_N), \quad \sigma(0) = \sigma_0, \tag{3}$$

where $\phi(\cdot)$ is some appropriately chosen function of the state vectors $x_1, x_2, \ldots, x_N$ of all oscillators in the network and σ_0 is some initial condition on the evolution of $\sigma(t)$.

The strategy described by Equations (2) and (3) is a *global, centralized adaptive strategy* where the adaptation mechanism is selected globally for all oscillators in the networks. Specifically, we assume that the unique adaptive gain, equal for all oscillators, is adapted in a centralized manner on the basis of information on all the oscillators in the network.

An alternative approach is to consider a *local, decentralized strategy* where, in general, the network can be described as

$$\frac{\mathrm{d}x_i}{\mathrm{d}t} = f(x_i) - \sum_{j=1}^{N}\sigma_{ij}(t)\mathcal{L}_{ij}h(x_j), \quad i = 1, 2, \ldots, N, \tag{4}$$

with $\sigma_{ij}(t)$ being the adaptive gains associated with each of the edges between different nodes i and j. Each of the adaptive gains is then associated with an adaptive law of the form

$$\dot{\sigma}_{ij}(t) = \phi_{ij}(I(x_i, x_j)), \quad \sigma_{ij}(0) = \sigma_{ij}^0, \tag{5}$$

where $\phi_{ij}(\cdot)$ is now some appropriately chosen local function, $I(x_i, x_j)$ represents the neighbourhood of the nodes i and j, and σ_{ij}^0 are the initial conditions on each of the adaptive gains in the network. We will also consider the case where different coupling gains are associated to each node in the network.

Using this general framework, in this paper, we will propose a different adaptation mechanism that involves different choices for the function ϕ and ϕ_{ij} in Equations (3)–(5).

2.1. *Global adaptive strategies*

First, we consider a centralized strategy: the gain σ is time-varying and its derivative is chosen adaptively on the basis of global information on the whole network. The chosen adaptation law is the following:

$$\dot{\sigma}(t) = \frac{\mu}{N}\sum_{j=1}^{N}\left\|h(x_j(t)) - m(t)\right\| := \Phi(t), \tag{6}$$

where

$$m(t) = \frac{\sum_{j=1}^{N}h(x_j)}{N}. \tag{7}$$

As shown in Equations (6) and (7), the rate of change of σ is selected according to the average distance between the node output $h(x_j)$ and the quantity m computed by summing the outputs of all nodes in the network.

In networks with non-homogeneous node degrees (for instance, scale-free networks), a convenient strategy might be to adapt only those gains associated with the nodes with the highest degree (the hubs).

The adaptation law then becomes

$$\dot{\sigma}^{(i)}(t) := \begin{cases} \Phi(t) & \text{if } i \in H, \\ 0 & \text{otherwise,} \end{cases} \tag{8}$$

where H is the set of the hubs of the network.

2.2. *Local adaptive strategies*

We isolate two possible alternative local adaptive strategies for networks synchronization: (1) *vertex-based*, where the same adaptive gain is associated with all edges incoming in a given node; and (2) *edge-based* where an adaptive gain is associated with every link in the network.

Namely, we have the following two approaches.

(1) *Vertex-based*. An adaptive gain $\sigma_i(t)$ is associated with every vertex $i = 1, \ldots, N$. Namely, the adaptation law is set to:

$$\dot{\sigma}_i(t) = \mu \left\| \sum_{j \in V_i} (h(x_j) - h(x_i)) \right\| := \Phi_i(t), \tag{9}$$

where V_i is the set of neighbours of the node i. Another simple vertex-based strategy is the one proposed by Kurths and Zhou in [6], given by

$$\dot{\sigma}_i(t) = \frac{\mu \Delta_i}{(1 + \Delta_i)}, \quad \mu > 0, \tag{10}$$

where

$$\Delta_i = \left| h(x_i) - \left(\frac{1}{k_i} \right) \sum_{j=1}^{N} A_{ij} h(x_j) \right|. \tag{11}$$

(2) *Edge-based*. An adaptive gain $\sigma_{ij}(t)$ is associated with each link. The dynamic of each $\sigma_{ij}(t)$ is described by the following differential equation:

$$\dot{\sigma}_{ij}(t) = \alpha \left\| (h(x_j) - h(x_i)) \right\| := \Phi_{ij}(t). \tag{12}$$

The idea behind the vertex-based approach is for each node to negotiate an appropriate coupling strength with all of its neighbours by comparing its output with that of all neighbouring nodes. Hence, an adaptive gain σ_i is associated with each node. The edge-based approach is instead based on the negotiation between each pair of nodes in the network. Basically, two neighbouring nodes compare their outputs and select their mutual coupling gain according to the relative distance between their outputs. In so doing, a different adaptive gain is associated with each link in the network.

To validate the strategies described above and evaluate their performance, we consider the problem of synchronizing a network of $N = 100$ oscillators, with all the adaptive gains starting

from zero initial values. We consider three types of oscillators at the nodes:

- identical Kuramoto oscillators;
- identical Rössler oscillators (with different state couplings);
- non-identical oscillators (Kuramoto and Rössler).

Also we repeat our simulations for three different network topologies: (1) Barabàsi–Albert scale-free (SF) networks; (2) small-world (SW) networks; and (3) random networks (for further details on these topologies, see [1,9,13]).

For the sake of brevity, we present below the results only for the more relevant local, decentralized adaptive strategies. Synchronization can also be successfully achieved using global, centralized strategies.

3. Adaptive synchronization of a network of identical Kuramoto oscillators

We consider networks of Kuramoto oscillators which were proposed as viable paradigmatic examples of synchronization of dynamical systems [5]. The long-term dynamics of any system of nearly identical, weakly coupled limit-cycle oscillators can be described by the following equation:

$$\dot{\theta}_i = \omega_i + \frac{K}{N}\sum_{j=1}^{N}\Gamma_{ij}(\theta_j - \theta_i), \quad i = 1, \ldots, N.$$

We can recast the governing equations of the model in terms of the following order parameter [5]:

$$re^{i\psi} = \frac{1}{N}\sum_{j=1}^{N} e^{i\theta_j}. \tag{13}$$

The modulus r of the order parameter is a measure of synchrony in the system, and the phase ψ gives the average phase of all the oscillators.

The governing equations in terms of the order parameter are

$$\dot{\theta}_i = \omega_i + Kr\sin(\psi - \theta_i), \quad i = 1, \ldots, N.$$

Without the loss of generality, in our numerical analysis, we set $\omega = 0$ and we choose the initial conditions, $\theta_i(0)$, of the oscillators randomly from a standard normal distribution.

3.1. *Vertex-based strategy*

Adopting the strategy described by Equation (9) and replacing the norm by the absolute value, the equations of the whole network become

$$\dot{\theta}_i = \omega + \sigma_i\sum_{j=1}^{N} A_{ij}(\theta_j - \theta_i), \tag{14}$$

$$\dot{\sigma}_i = \mu\left|\sum_{j\in V_i}(\theta_j - \theta_i)\right|. \tag{15}$$

We consider an SF network generated using the Barabàsi–Albert method with an average degree equal to 10. Figures 1 and 2 show the synchronization dynamics of the network. We observe that, as the adaptive gains converge towards their constant finite steady-state values, the strategy is

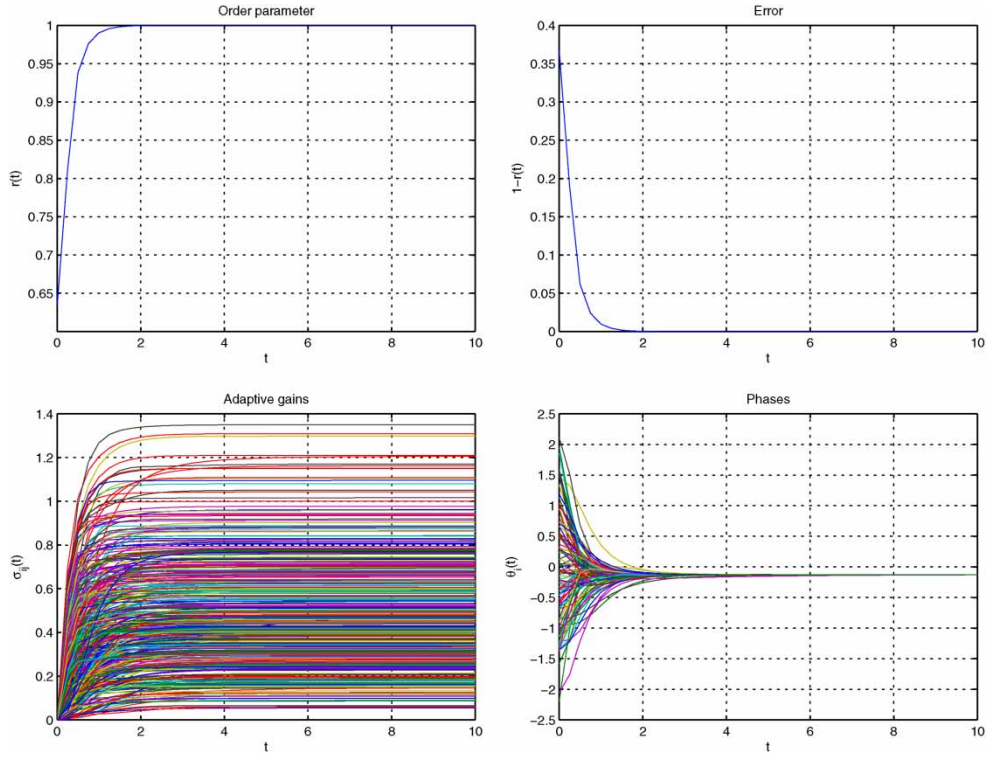

Figure 1. Evolution of order parameter (top left-hand panel), error (top right-hand panel), σ (bottom left-hand panel), and phases (bottom right-hand panel) in a BA network using the vertex-based strategy.

successful in synchronizing all oscillators on a common evolution. In particular, we observe that the order parameter converges towards unity, indicating that the synchronization error is going to be zero with all oscillator phases tending towards a common evolution within time $t = 2$. Figure 3 shows that by increasing the value of μ (i.e. increasing the rate of growth of σ), we reach the synchronous state in a shorter time.

Similar results are obtained by considering network of the same size, but with different topology (small-world and random), as shown in Figures 4–7.

3.2. *Edge-based strategy*

Now, if we choose the edge-based strategy described in Equation (12), the equations describing the network are the following:

$$\dot{\theta}_i = \omega + \sum_{j \in V_i} \sigma_{ij} \bullet A_{ij}(\theta_j - \theta_i), \tag{16}$$

$$\dot{\sigma}_{ij} = \alpha|\theta_j - \theta_i|, \tag{17}$$

where we set $\alpha = 0.1$ and $\bullet$ is the Hadamard product [4]. As shown in Figures 8 and 9, with an edge-based strategy, synchronization is also achieved, but the transition to synchrony is slower. This can be explained by noticing that in the edge-based case, the rate of change of the coupling gain is in general smaller and hence the growth of the coupling gains from their zero initial conditions is typically slower (see Figure 8).

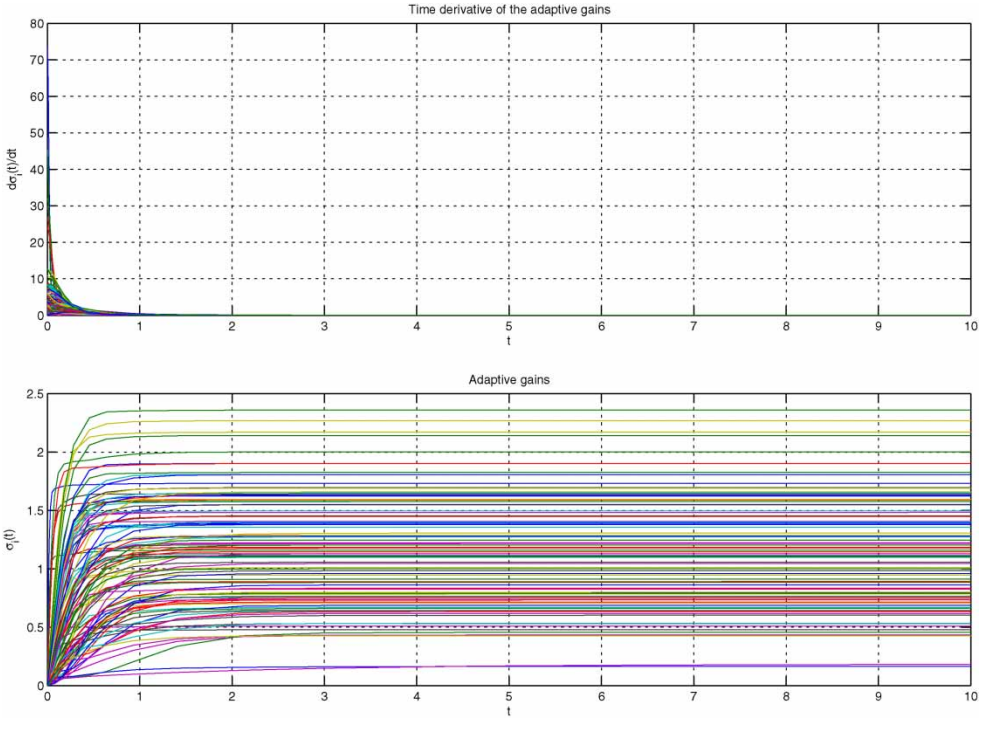

Figure 2. Evolution of $\dot{\sigma}$ (top), and σ (bottom) in a BA network using the vertex-based strategy.

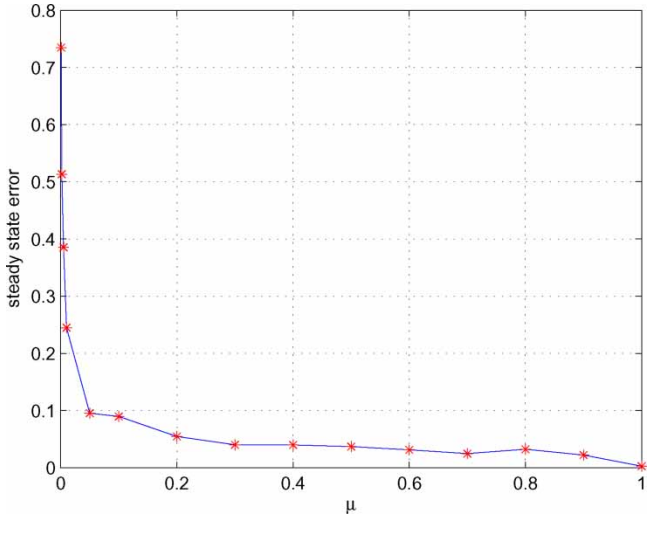

Figure 3. Error *vs*. gain μ in a BA network using the vertex-based strategy.

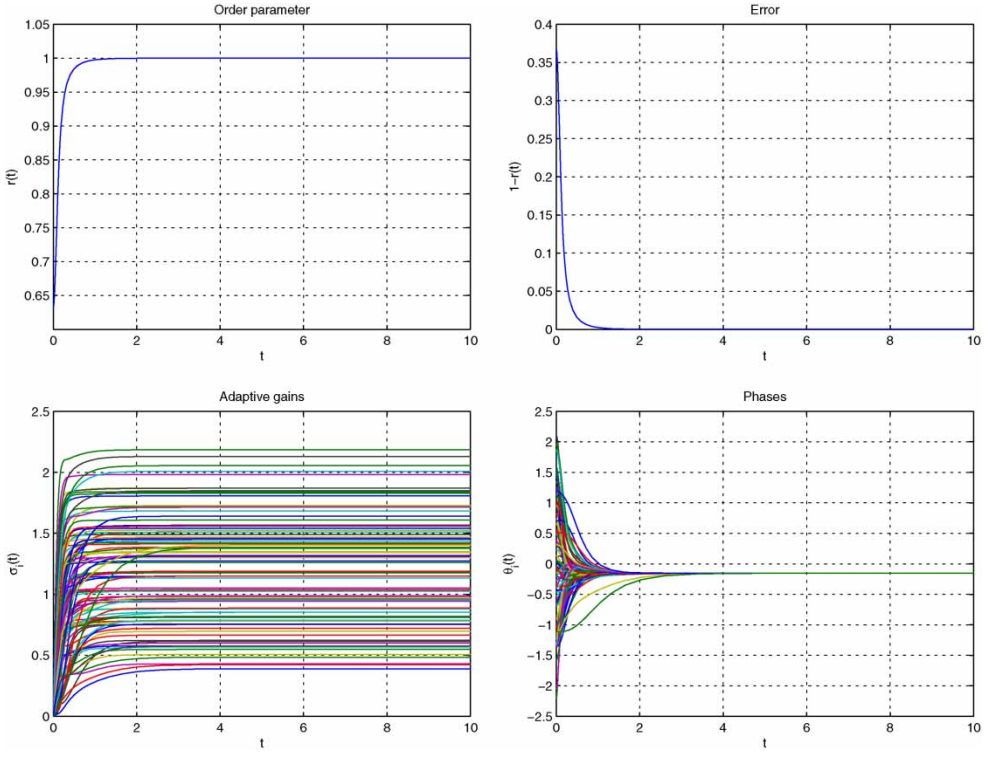

Figure 4. Evolution of order parameter (top left-hand panel), error (top right-hand panel), σ (bottom left-hand panel), and phases (bottom right-hand panel) in an SW network using the vertex-based strategy.

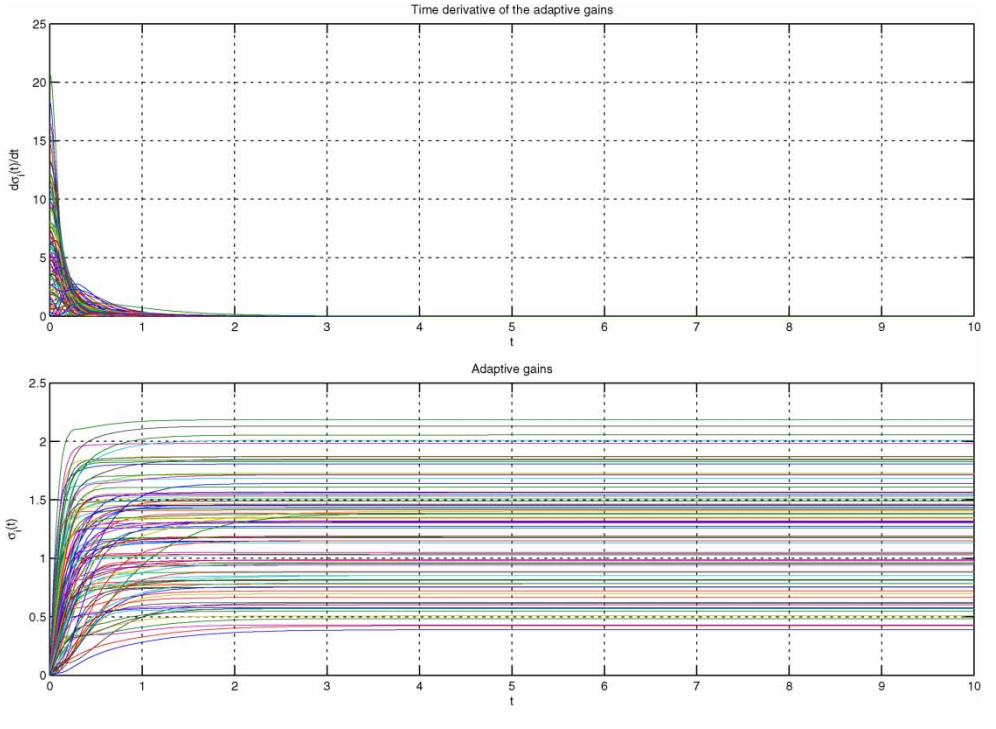

Figure 5. Evolution of $\dot{\sigma}$ (top) and σ (bottom) in an SW network using the vertex-based strategy.

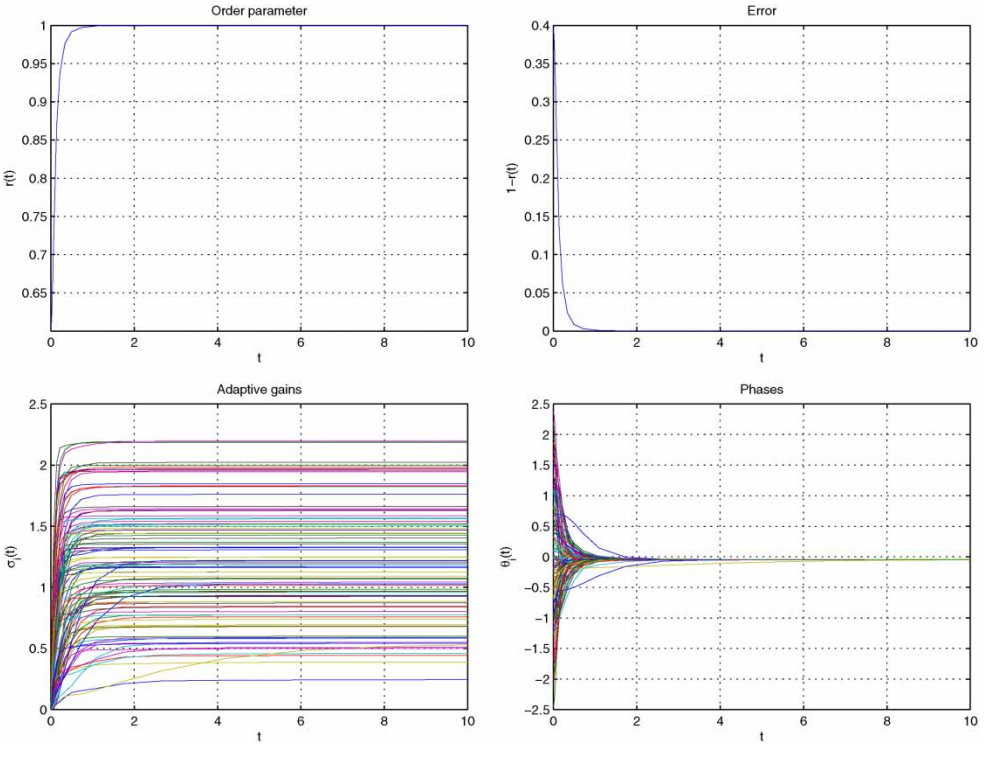

Figure 6. Evolution of order parameter (top left-hand panel), error (top right-hand panel), σ (bottom left-hand panel), and phases (bottom right-hand panel) in a random network using the vertex-based strategy.

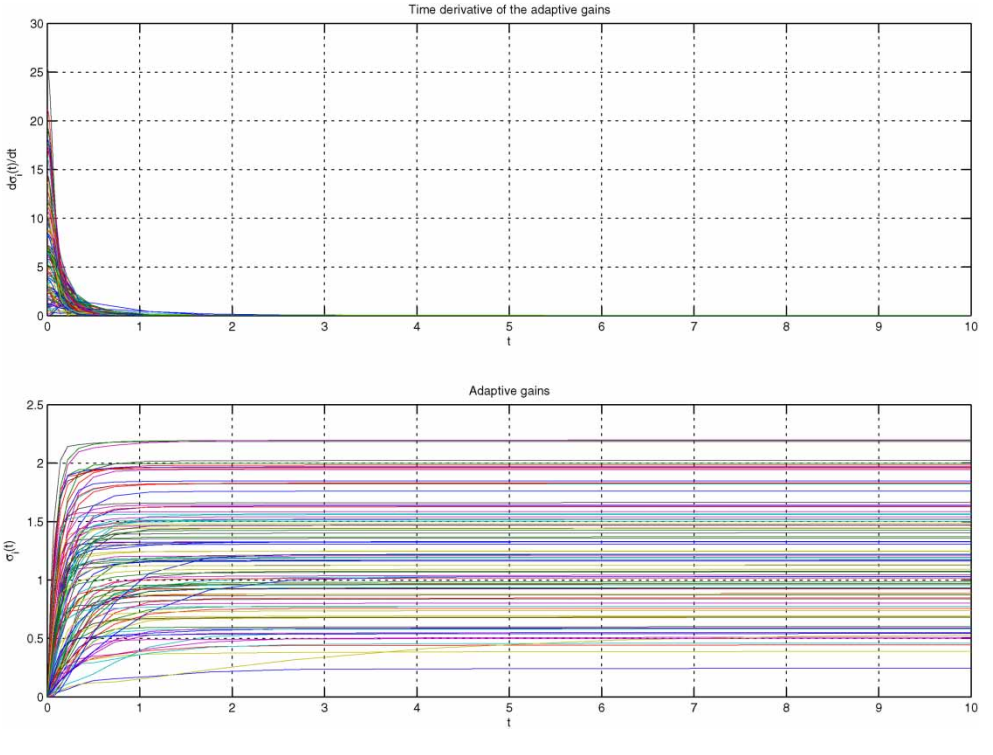

Figure 7. Evolution of $\dot{\sigma}$ (top) and σ (bottom) in a random network using the vertex-based strategy.

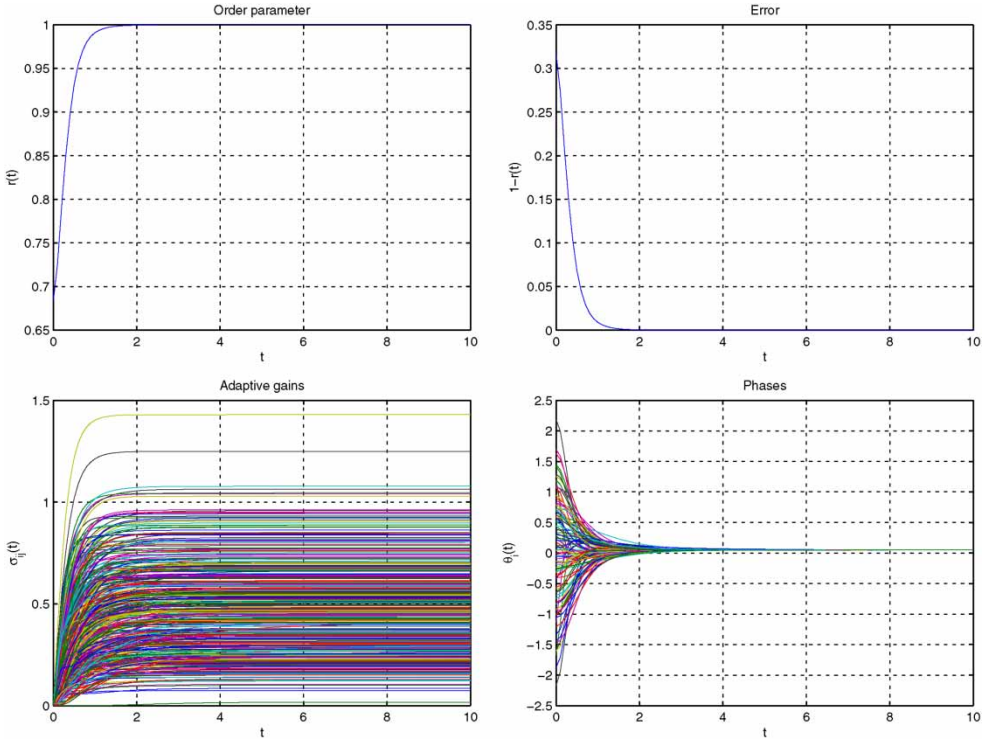

Figure 8. Evolution of order parameter (top left-hand panel), error (top right-hand panel), σ (bottom left-hand panel), and phases (bottom right-hand panel) in a BA network using the edge-based strategy.

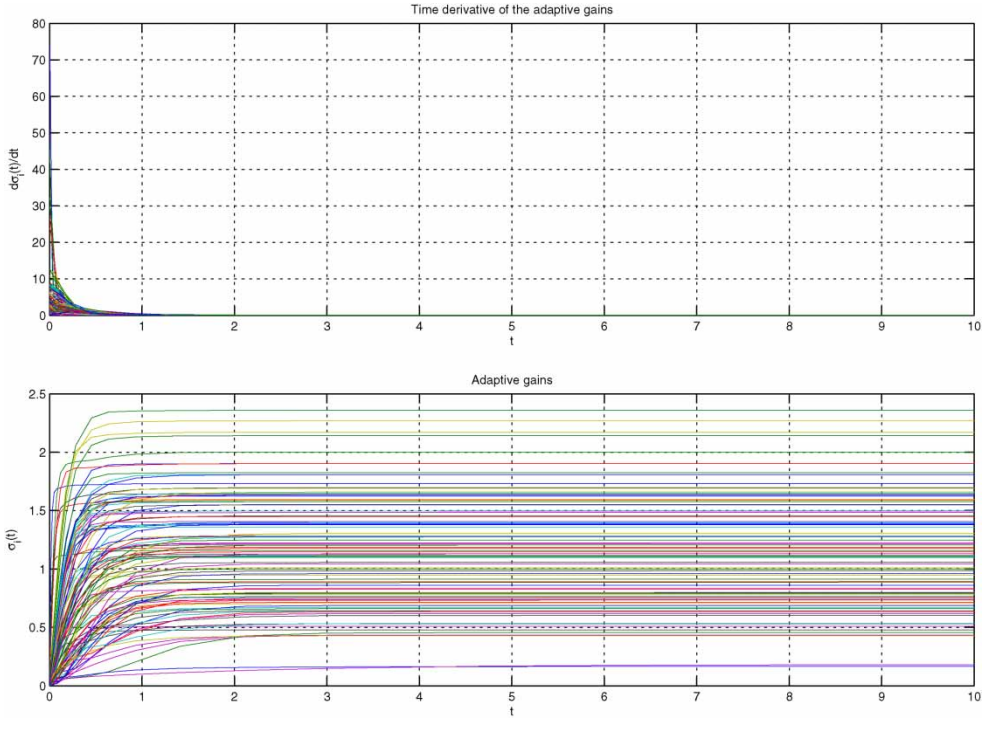

Figure 9. Evolution of $\dot{\sigma}$ (top) and σ (bottom) in a BA network using the edge-based strategy.

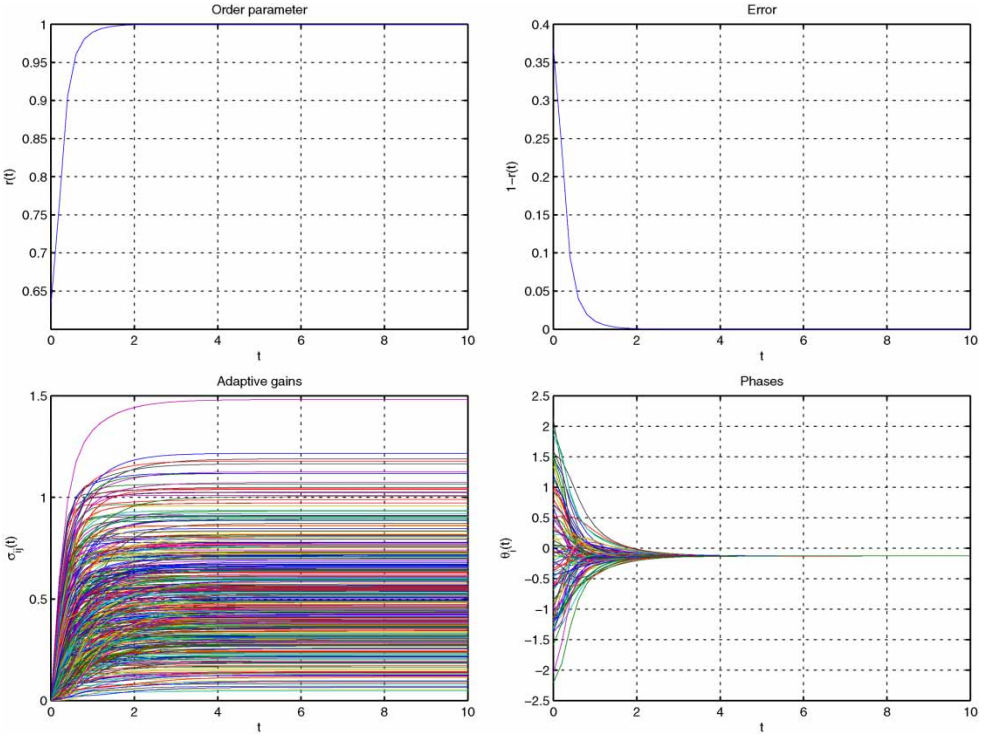

Figure 10. Evolution of order parameter (top left-hand panel), error (top right-hand panel), σ (bottom left-hand panel), and phases (bottom right-hand panel) in an SW network using the edge-based strategy.

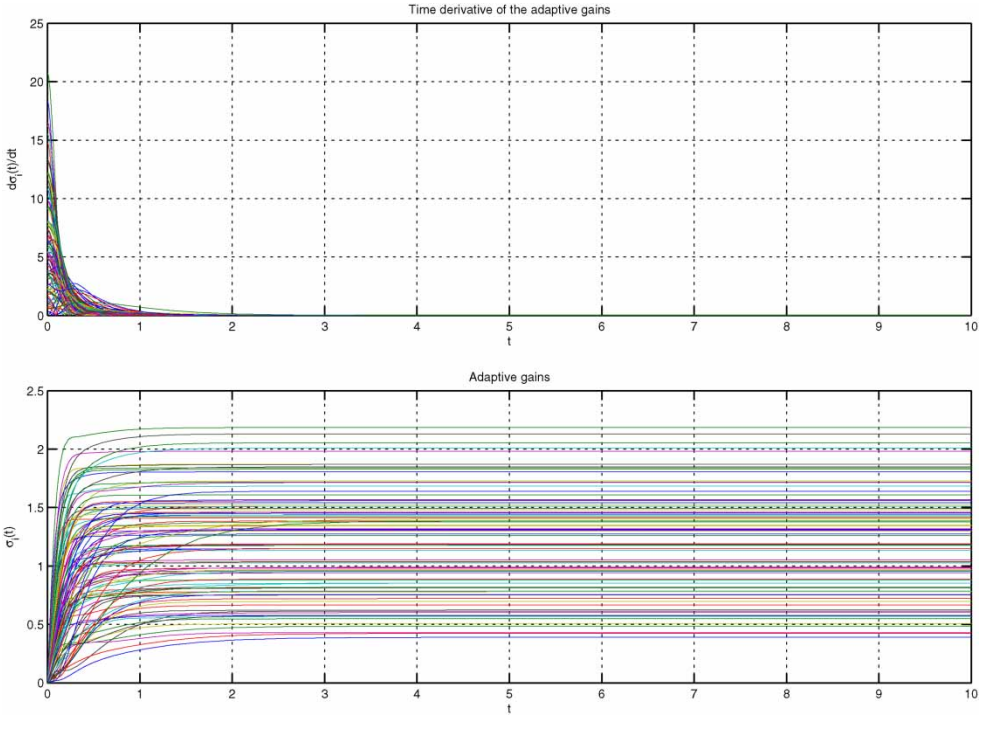

Figure 11. Evolution of $\dot{\sigma}$ (top) and σ (bottom) in an SW network using the edge-based strategy.

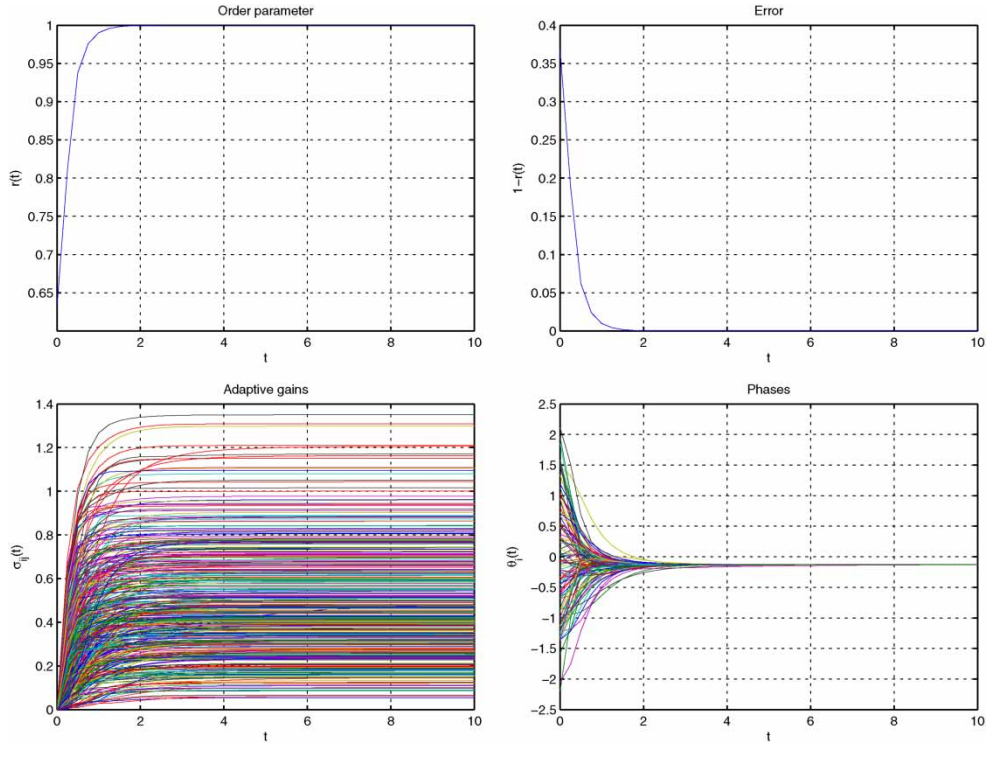

Figure 12. Evolution of order parameter (top left-hand panel), error (top right-hand panel), σ (bottom left-hand panel), and phases (bottom right-hand panel) in a random network using the edge-based strategy.

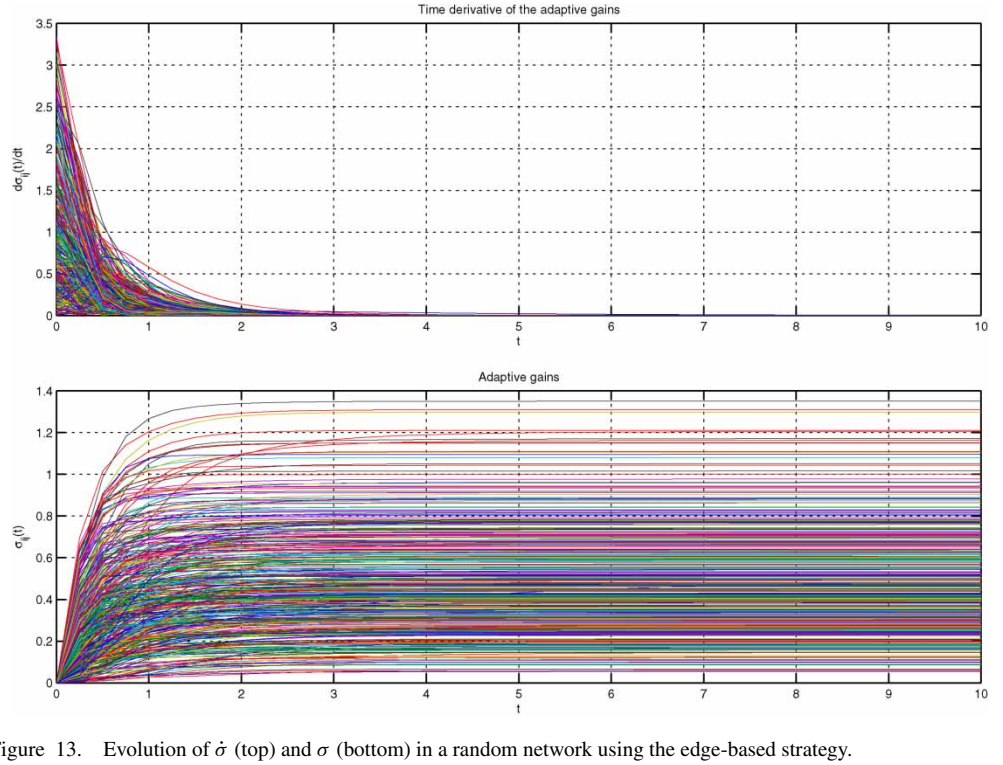

Figure 13. Evolution of $\dot{\sigma}$ (top) and σ (bottom) in a random network using the edge-based strategy.

Similar behaviour is observed when the underlying network topology is changed to small-world or random as shown in Figures 10–13.

The case considered so far is that of identical Kuramoto oscillators. Actually, by setting ω to zero, we considered a classical consensus problem in control theory where the oscillators are coupled linearly through the edges of the network [10]. We now move to the case of a more complex dynamical system at the nodes. Namely, we choose Rössler systems at the nodes, which are typically used in the synchronization literature as a suitable representative testbed case for chaotic synchronization strategies.

4. Adaptive synchronization of a network of identical Rössler oscillators coupled through on the x-variable

The Rössler system is described by a set of three non-linear ODEs [11]. These differential equations define a continuous-time dynamical system that may exhibit chaotic dynamics. The defining equations are

$$\dot{x} = -y - z, \tag{18}$$

$$\dot{y} = x + ay, \tag{19}$$

$$\dot{z} = b + z(x - c). \tag{20}$$

In what follows, we set $a = 0.1$, $b = 0.1$, and $c = 14$. With this choice of the parameters, the behaviour of the uncoupled Rössler system is chaotic. As mentioned earlier, the initial conditions of the state variables of the system are chosen randomly from a standard normal distribution.

4.1. *Vertex-based strategy*

In their recent work, Kurths and Zhou [6] apply an adaptive strategy [see Equations (10) and (11)] to a scale-free network of identical Rössler systems. In this subsection, we compare their strategy to the one described in Equation (9).

To make this comparison, we opt for a BA network with an average degree equal to 10.

The equations of the network are

$$\dot{x}_i = F_x(x_i, y_i, z_i) + \sigma_i \sum_{j=1}^{N} A_{ij}(x_j - x_i), \tag{21}$$

$$\dot{y}_i = F_y(x_i, y_i, z_i), \tag{22}$$

$$\dot{z}_i = F_z(x_i, y_i, z_i), \tag{23}$$

where $F(x_i, y_i, z_i) = [F_x(x_i, y_i, z_i), F_y(x_i, y_i, z_i), F_z(x_i, y_i, z_i)]$ is the vector field describing the dynamics of each oscillator.

Adopting the strategy by Kurths and Zhou, we have

$$\dot{\sigma}_i = \mu \frac{\Delta_i}{1 + \Delta_i}, \quad i = 1, \ldots, N, \tag{24}$$

where Δ_i is the *distance* of node i from the 'mean activity' of its neighbours [6], defined as

$$\Delta_i = \left| x_i - \left(\frac{1}{k_i}\right) \sum_{j=1}^{N} A_{ij} x_j \right|. \tag{25}$$

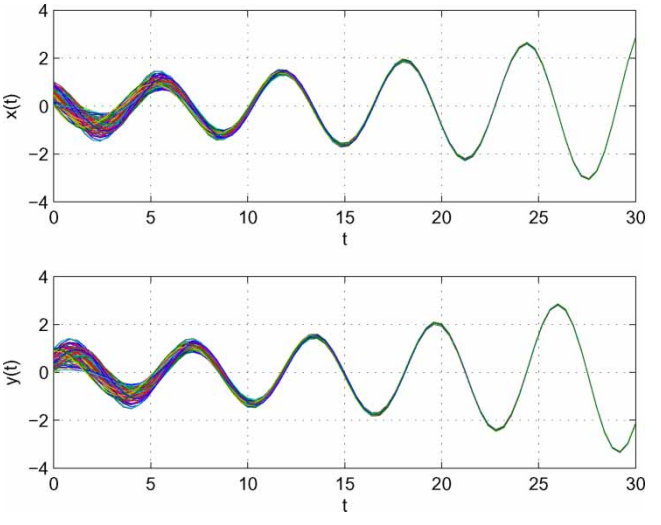

Figure 14. Evolution of x (top) and y (bottom) in a BA network adopting the strategy presented in [6].

Using the strategy proposed in this paper, we would simply set the gain adaptation law to

$$\dot{\sigma}_i = \mu \left| \sum_{j \in V_i} (x_j - x_i) \right|, \tag{26}$$

where μ is set equal to 0.1. Note that the major difference between the two strategies is that in Equation (24), the rate of change of the adaptive gain is upper bounded by μ as Δ_i becomes larger.

As we can see comparing Figures 14 and 15 with Figures 16 and 17, synchronization is achieved with both adaptation strategies with the transient dynamics being qualitatively the same. However,

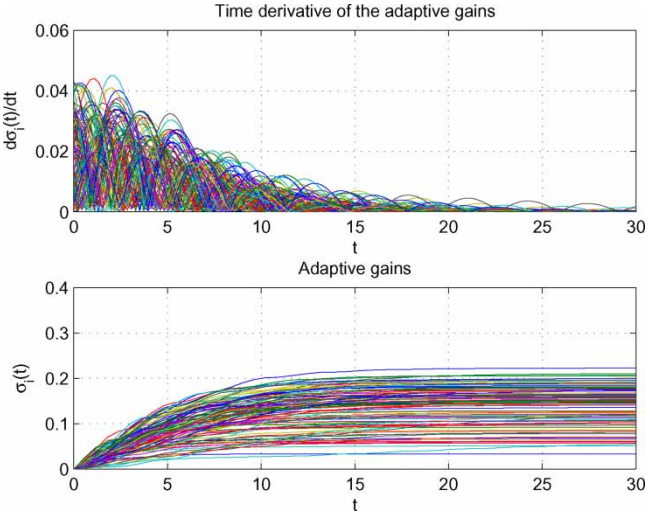

Figure 15. Evolution of σ (top) and $\dot{\sigma}$ (bottom) in a BA network adopting the strategy presented in [6].

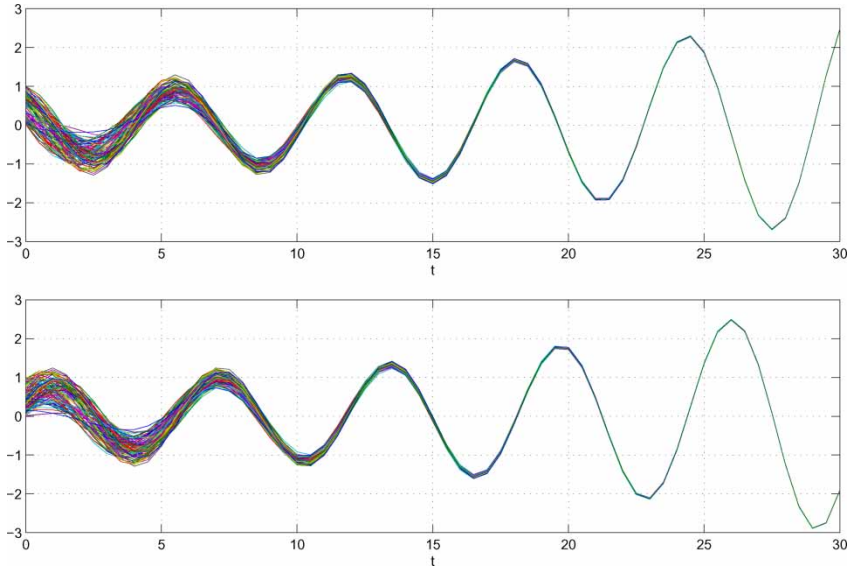

Figure 16. Evolution of x (top) and y (bottom) in a BA network using the vertex-based strategy.

we notice that the former strategy allows us to reach synchronization with a lower overall control effort as the adaptation rate of the coupling gain is upper bounded.

Similar results are obtained when the network topology is varied to small-world or random. For the sake of brevity, we omit here the corresponding figures as the dynamics are qualitatively the same as those observed in the case of scale-free networks.

We now move to the case of the edge-based strategy.

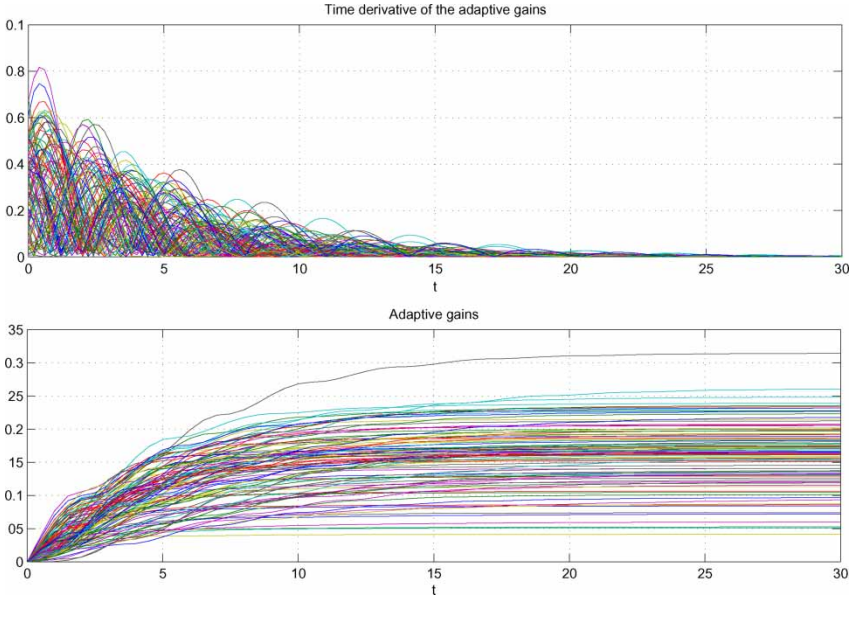

Figure 17. Evolution of σ (top) and $\dot{\sigma}$ (bottom) in a BA network using the vertex-based strategy.

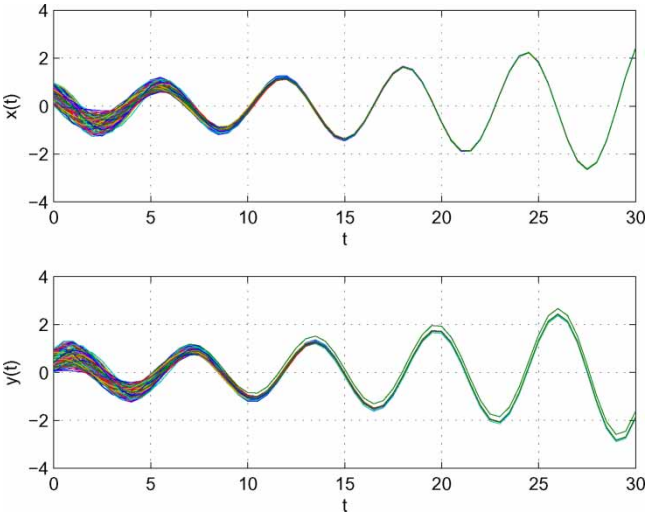

Figure 18. Evolution of x (top) and y (bottom) in a BA network using the edge-based strategy.

4.2. *Edge-based strategy*

The governing equations of the network could be rewritten as follows:

$$\dot{x}_i = F_x(x_i, y_i, z_i) + \sum_{j=1}^{N} A_{ij}\sigma_{ij}(x_j - x_i), \tag{27}$$

$$\dot{y}_i = F_y(x_i, y_i, z_i), \tag{28}$$

$$\dot{z}_i = F_z(x_i, y_i, z_i), \tag{29}$$

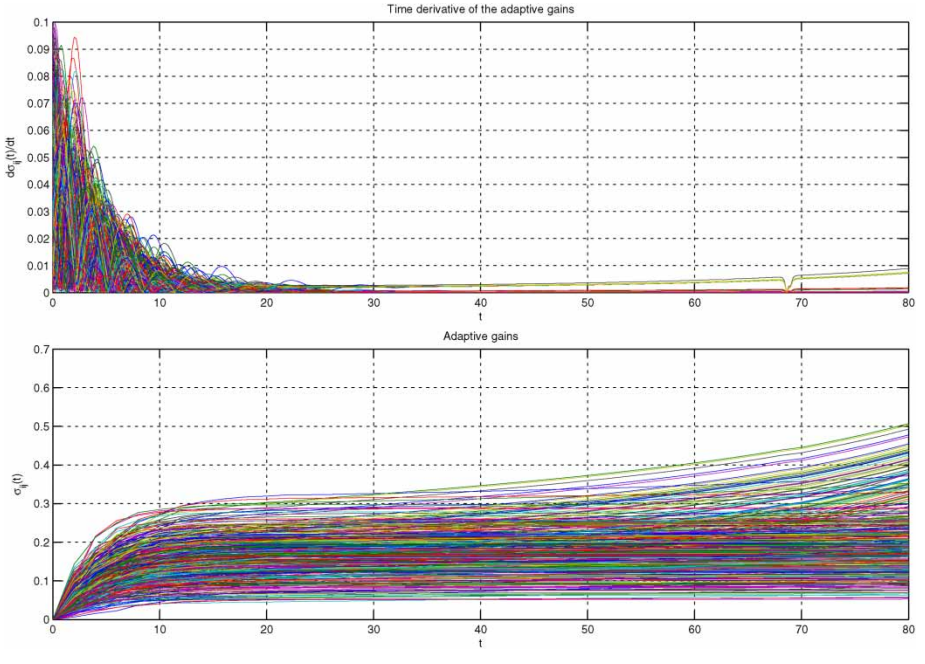

Figure 19. Evolution of σ (top) and $\dot{\sigma}$ (bottom) in a BA network using the edge-based strategy.

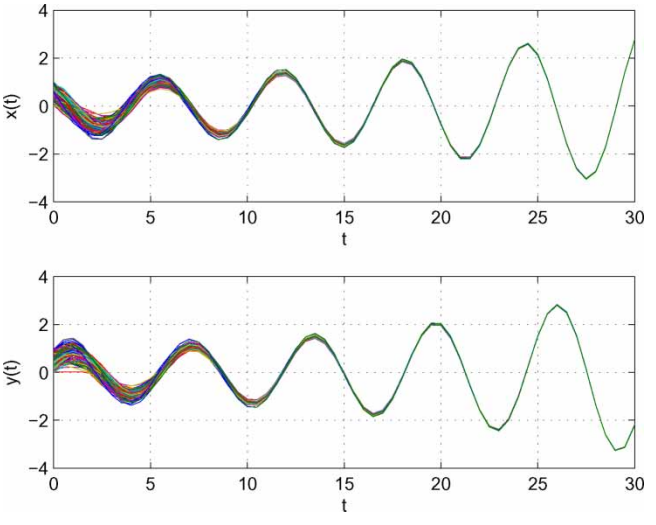

Figure 20. Evolution of x (top) and y (bottom) in an SW network using the edge-based strategy.

$$\dot{\sigma}_{ij} = \alpha |x_j - x_i|, \tag{30}$$

for $i = 1, \ldots, N$; $j : A_{ij} = 1$, where α is chosen equal to 0.1.

In this case, we observed dramatic effects of the network topology on the synchronization dynamics. In particular, as shown in Figures 18 and 19, when we consider a scale-free topology, the adaptive algorithm is unable to make the network synchronize with several gains diverging as time increases. The behaviour changes dramatically when the network topology is changed to small-world or random. As shown in Figures 20–23, in a random or a small-world network, the same strategy leads to complete synchronization. Moreover, the settling values of the σ_{ij} are in average lower than the σ_i in the vertex-based strategy.

Apart from the topology of the connections between nodes in the network, another important factor that has been already observed in the literature is the state coupling we have considered so far. In particular, we assumed that the Rössler are coupled to each other through the x-variable of their three-dimensional state vector. Obviously, better synchronization results can be expected if the oscillators are coupled through their entire state vector. This is precisely the case analyzed in the next section.

5. Adaptive synchronization of a network of identical Rössler oscillators coupled through all states

In the following simulation, we test our decentralized strategies on networks of identical Rössler systems coupled on all the three state variables.

5.1. *Vertex-based strategy*

Let us denote $w_i = (x_i, y_i, z_i)^{\mathrm{T}}$ the state of an individual Rössler oscillator. The governing equations become

$$\dot{w}_i = F(w_i) + \sigma_i \bullet \sum_{j=1}^{N} A_{ij}(w_j - w_i), \quad i = 1, \ldots, N, \tag{31}$$

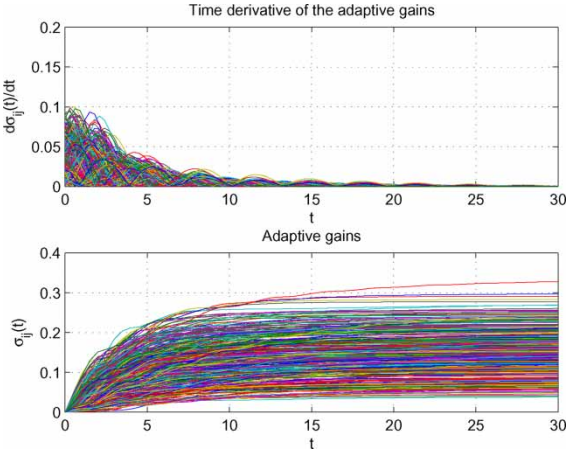

Figure 21. Evolution of σ (top) and $\dot{\sigma}$ (bottom) in an SW network using the edge-based strategy.

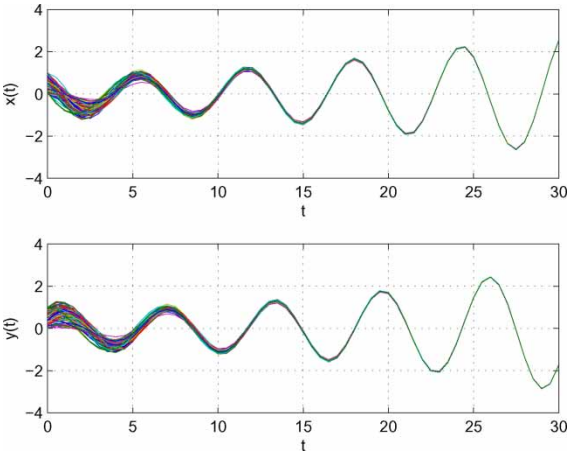

Figure 22. Evolution of x (top) and y (bottom) in a random network using the edge-based strategy.

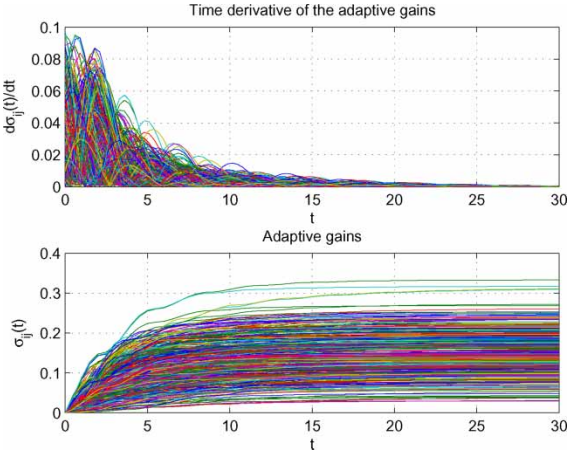

Figure 23. Evolution of σ (top) and $\dot{\sigma}$ (bottom) in a random network using the edge-based strategy.

where $F(w_i)$ is the dynamic of the ith oscillator, $\sigma_i = (\sigma_x^i, \sigma_y^i, \sigma_z^i)$, and $\bullet$ is the Hadamard product [4]. The equations of the dynamics of σ_i are as follows:

$$\dot{\sigma}_x^i = \mu \left| \sum_{j \in V_i} (x_j - x_i) \right|, \tag{32}$$

$$\dot{\sigma}_y^i = \mu \left| \sum_{j \in V_i} (y_j - y_i) \right|, \tag{33}$$

$$\dot{\sigma}_z^i = \mu \left| \sum_{j \in V_i} (z_j - z_i) \right|, \quad i = 1, \ldots, N. \tag{34}$$

In the simulations, we choose $\mu = 0.1$. Observing Figures 24–29, we can notice that synchronization is now always achieved through the same qualitative transient dynamics irrespective of the topology being considered. However, it is worth mentioning here that the synchronization of small-world and random networks is easier, in the sense that it seems to require lower control effort as the settling values of the σ_i are lower.

5.2. *Edge-based strategy*

Let us now consider a different $\sigma_{ij} = (\sigma_x^{ij}, \sigma_y^{ij}, \sigma_z^{ij})$, for each edge

$$\dot{w}_i = F(w_i) + \sum_{j=1}^{N} \sigma_{ij} \cdot A_{ij}(w_j - w_i), \tag{35}$$

$$\dot{\sigma}_x^{ij} = \alpha |x_j - x_i|, \tag{36}$$

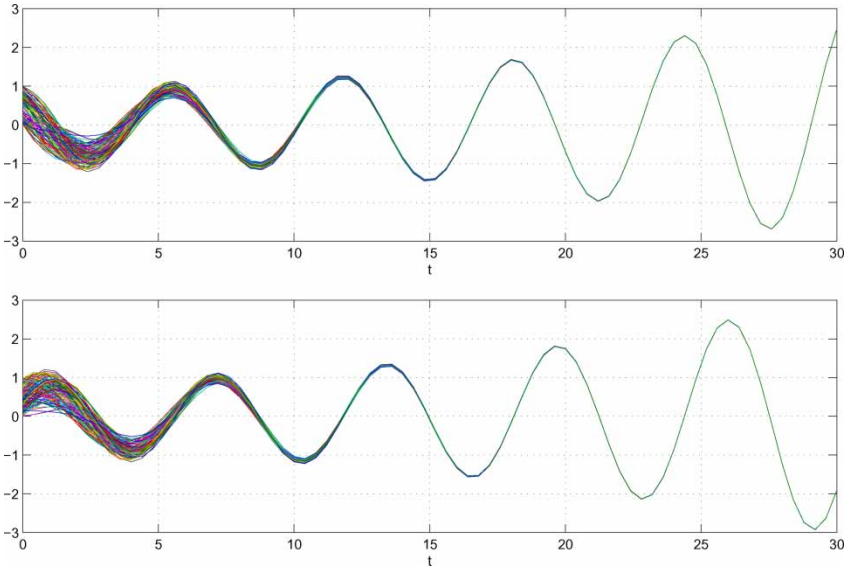

Figure 24. Evolution of x (top) and y (bottom) in a BA network using the vertex-based strategy.

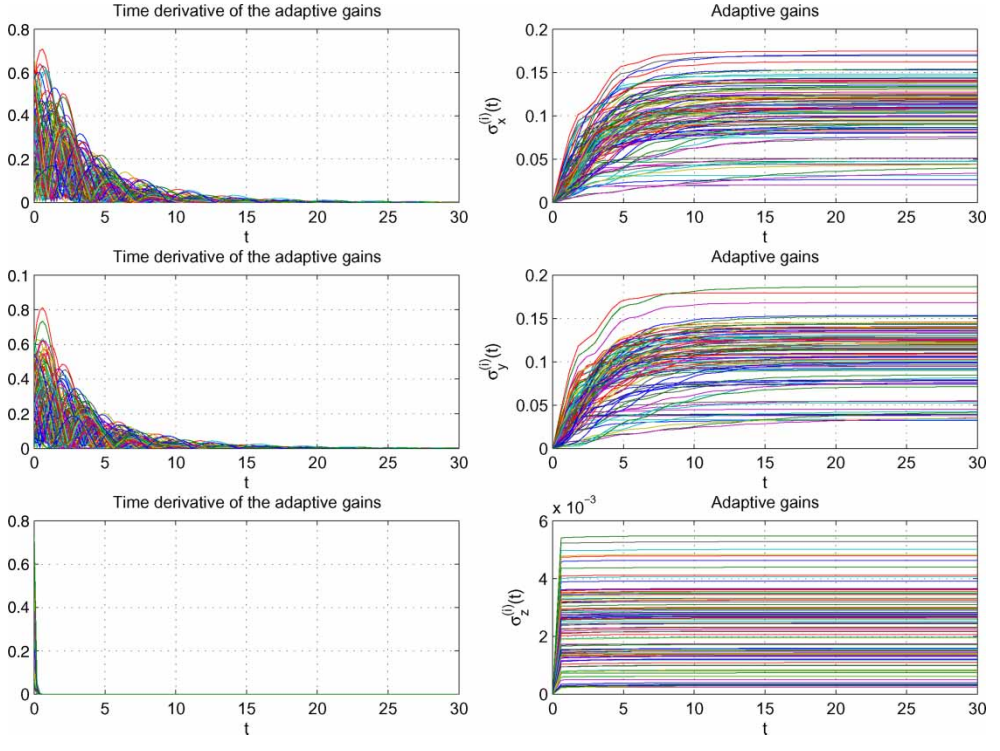

Figure 25. Evolution of σ (right-hand panel) and $\dot{\sigma}$ (left-hand panel) in a BA network using the vertex-based strategy.

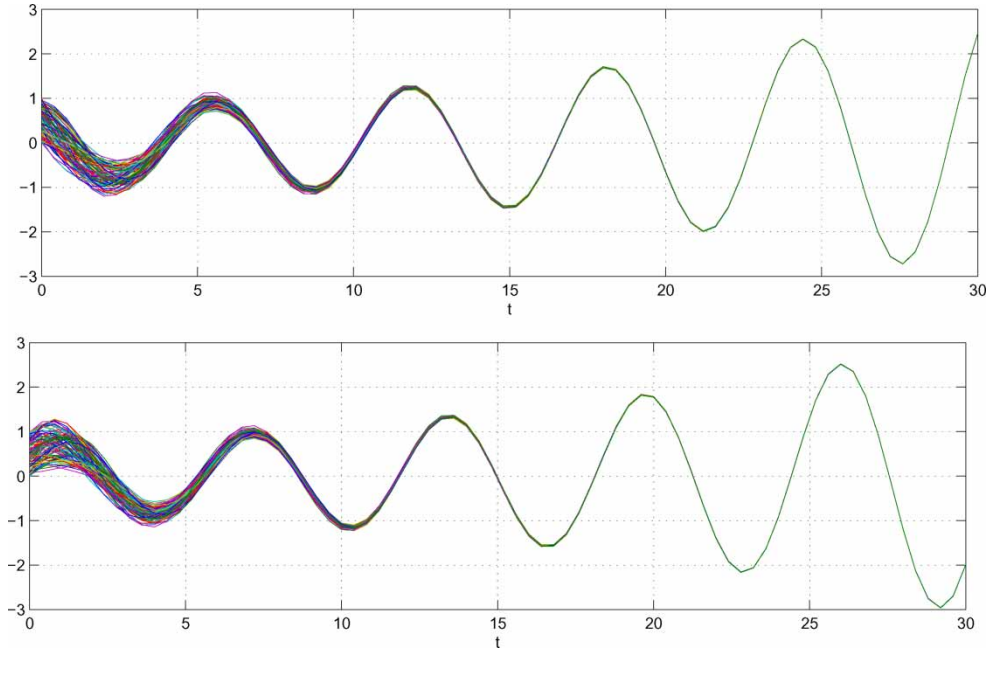

Figure 26. Evolution of x (top) and y (bottom) in an SW network using the vertex-based strategy.

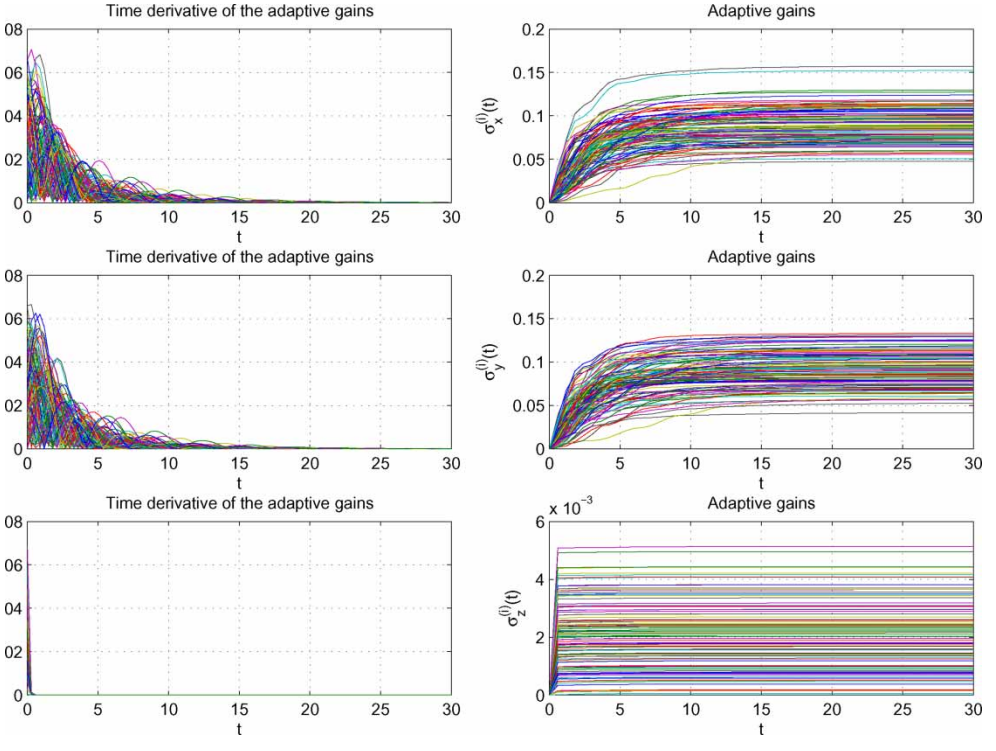

Figure 27. Evolution of σ (right-hand panel) and $\dot{\sigma}$ (left-hand panel) in an SW network using the vertex-based strategy.

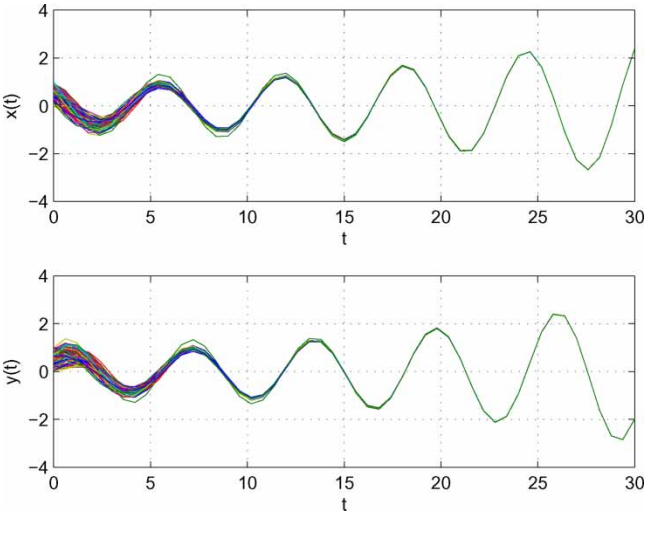

Figure 28. Evolution of x (top) and y (bottom) in a random network using the vertex-based strategy.

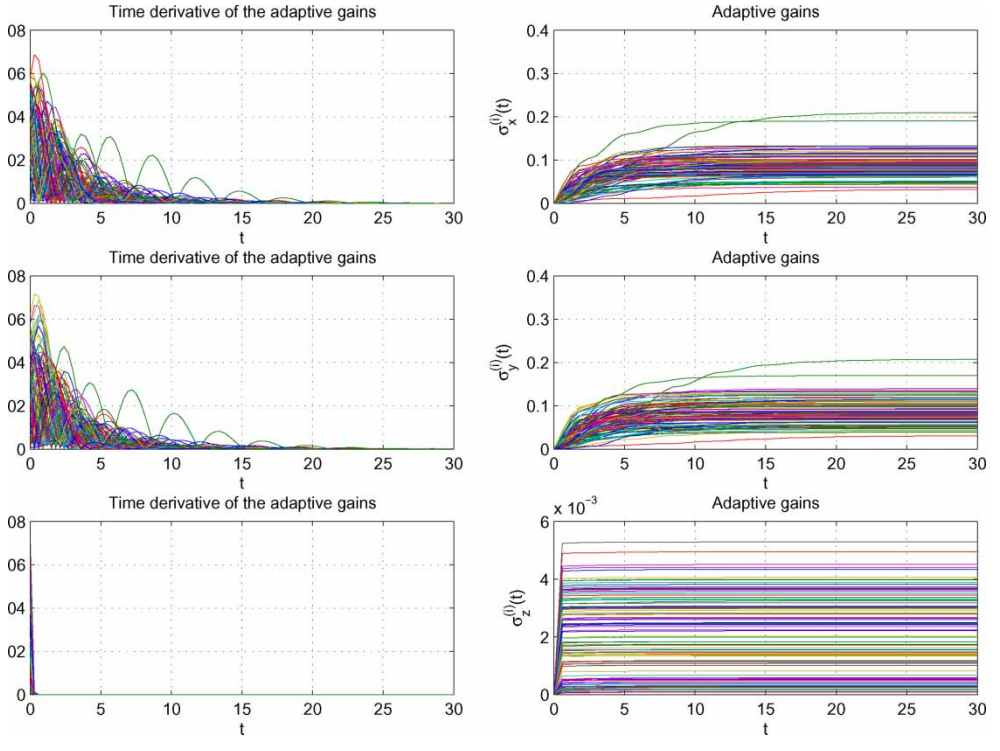

Figure 29. Evolution of σ (right-hand panel) and $\dot{\sigma}$ (left-hand panel) in a random network using the vertex-based strategy.

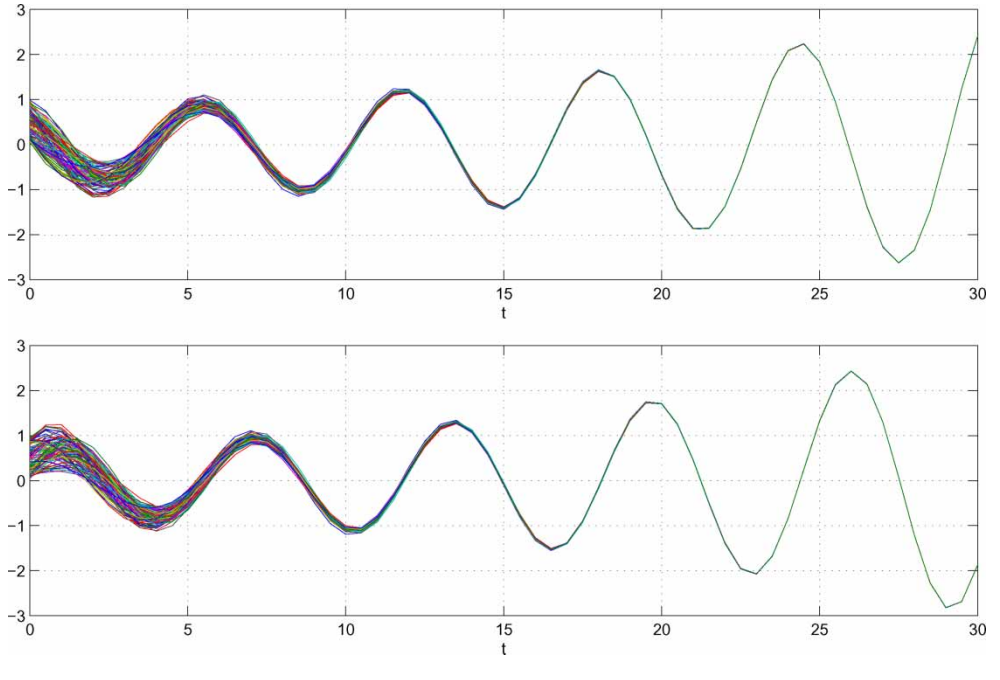

Figure 30. Evolution of x (top) and y (bottom) in a BA network using the edge-based strategy.

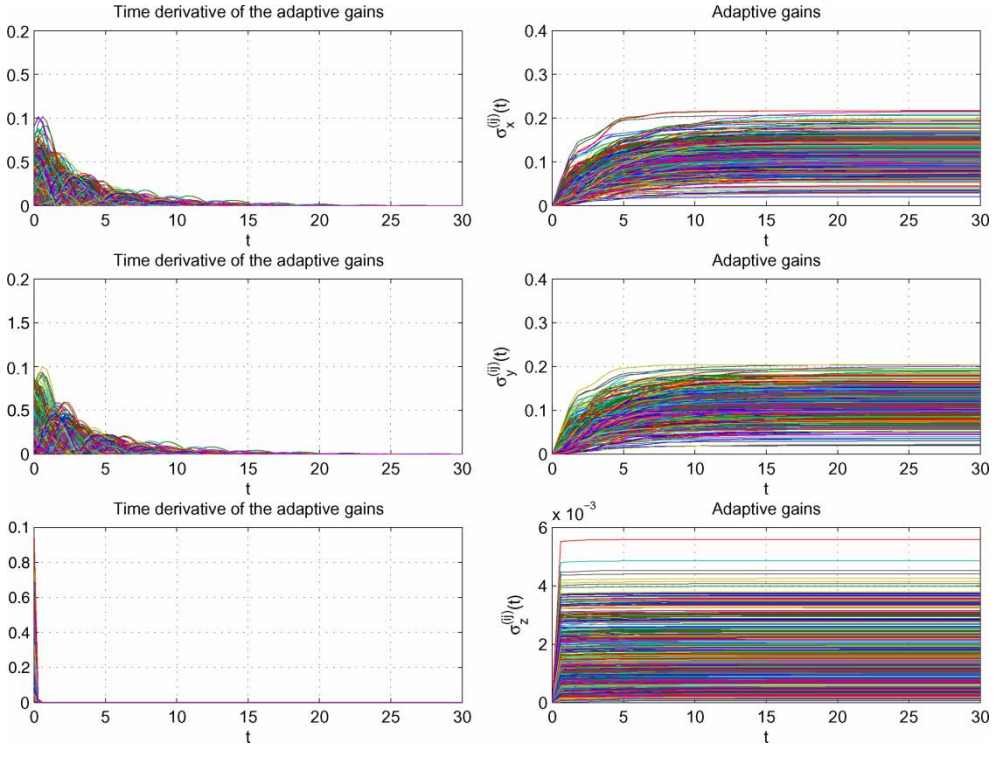

Figure 31. Evolution of σ (right-hand panel) and $\dot{\sigma}$ (left-hand panel) in a BA network using the edge-based strategy.

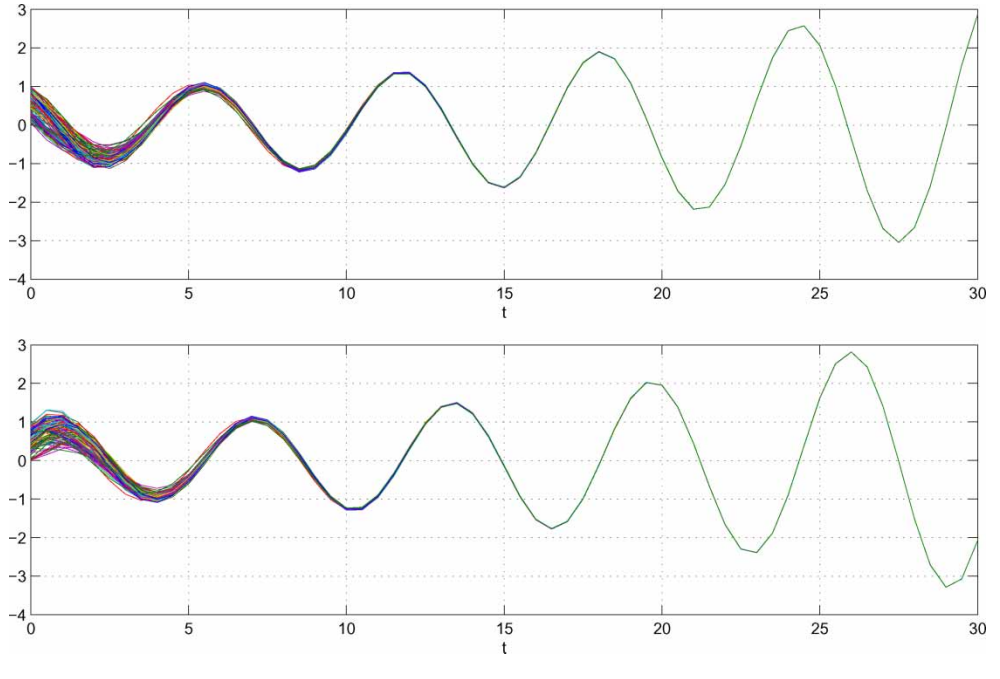

Figure 32. Evolution of x (top) and y (bottom) in an SW network using the edge-based strategy.

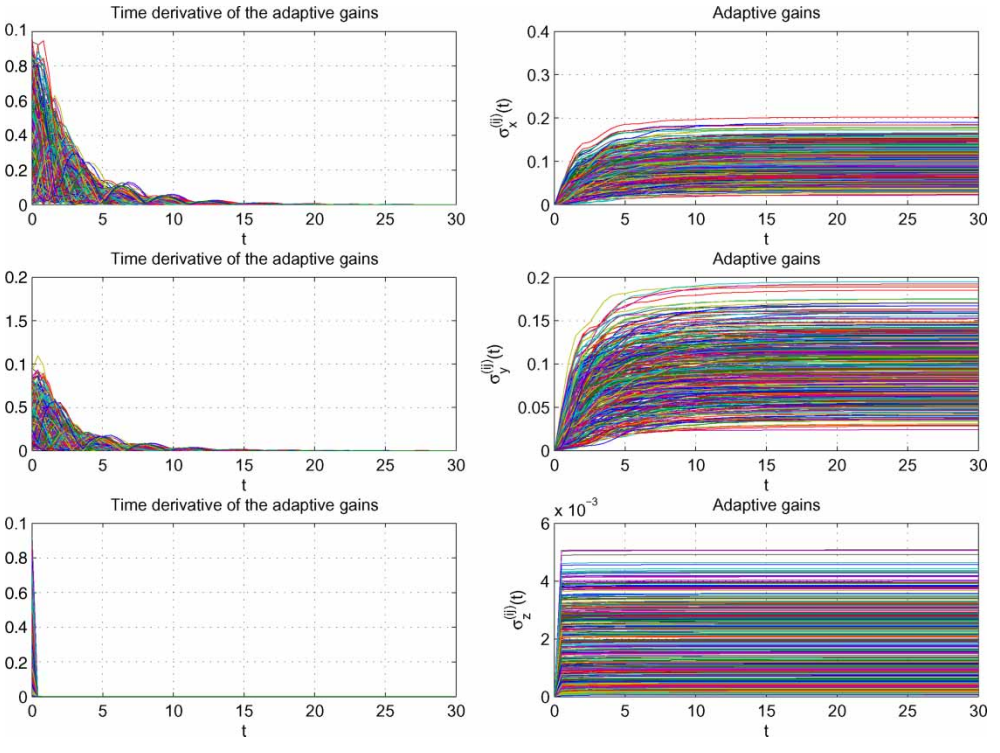

Figure 33. Evolution of σ (right-hand panel) and $\dot{\sigma}$ (left-hand panel) in an SW network using the edge-based strategy.

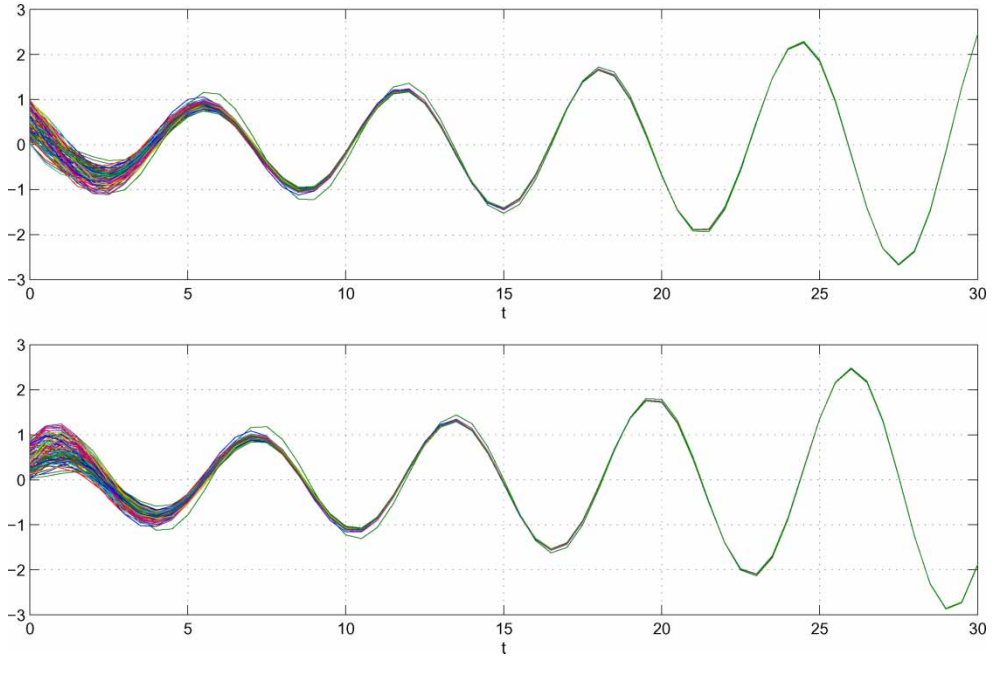

Figure 34. Evolution of x (top) and y (bottom) in a random network using the edge-based strategy.

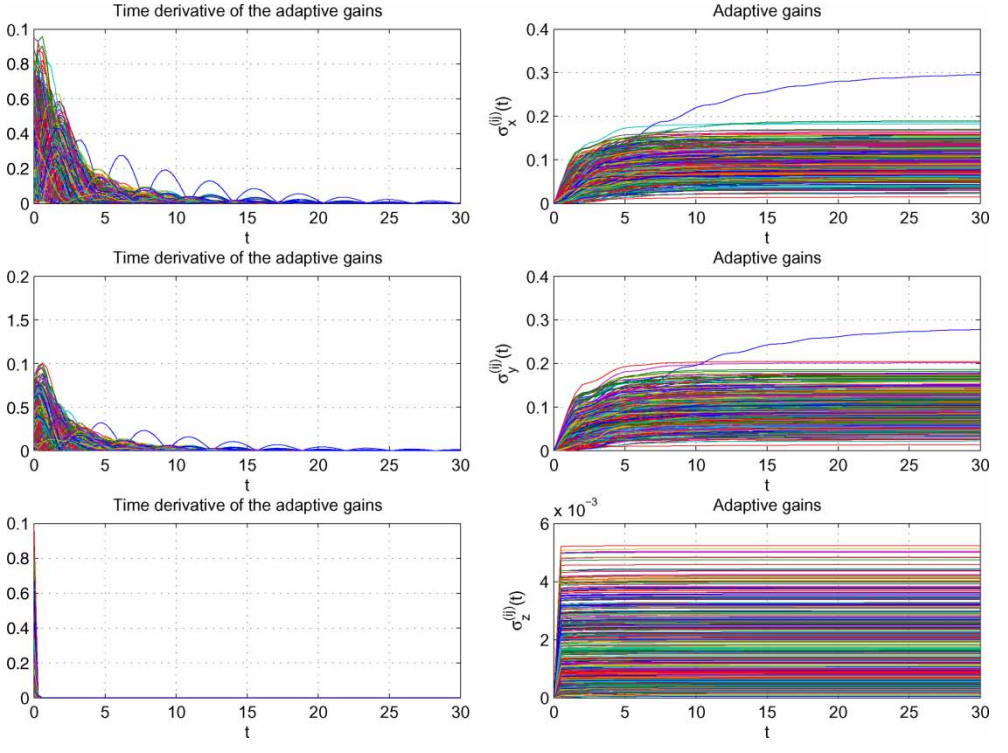

Figure 35. Evolution of σ (right-hand panel) and $\dot{\sigma}$ (left-hand panel) in a random network using the edge-based strategy.

$$\dot{\sigma}_y^{ij} = \alpha |y_j - y_i|, \tag{37}$$

$$\dot{\sigma}_z^{ij} = \alpha |z_j - z_i|, \tag{38}$$

for $i = 1, \ldots, N, \quad j : A_{ij} = 1$, where we set $\alpha = 0.1$.

As we can see in Figures 30–35, the synchronous state is always reached. For all different topologies, comparing these results with the one obtained with the vertex-based strategy, we can see that the time to synchronize is quite similar, but for the edge-based strategy the growth of the gains σ_{ij} is slower and their settling values smaller.

6. Discussion

Now, we present a comparison between the various strategies presented so far. To evaluate the speed of convergence, we define the following quantity:

$$\epsilon(t) = \sum_{i,j=1}^{N} \left\| x_i(t) - x_j(t) \right\|, \tag{39}$$

and we compare the time t_s it takes to fulfill the following conditions:

$$\epsilon(t_s) = 0.1\epsilon(0), \tag{40}$$

$$\epsilon(t_s) < 0.1\epsilon(0), \quad \forall t > t_s. \tag{41}$$

Although this is not a precise measure of the settling time, it gives an indication of the convergence speed of the various strategies. As we can see from Table 1, the vertex-based strategy is able to synchronize the various networks of Kuramoto oscillators faster than the edge-based. On the other hand, the vertex-based strategy requires a higher control effort, in fact the settling values of the different σ are in average more than two times higher.

As for the Rössler, we have to remark that:

(1) The two strategies are quite equivalent, with similar control efforts and with settling times slightly lower for the edge-based strategy. We observe that the edge-based is not able to synchronize the BA network, when the coupling is only on x.
(2) Among the various topologies, we can see that the BA network is the one with the highest convergence speed, whereas the small-world is the slowest one.

Table 2 shows the effects of increasing the network size N on our measure of the convergence speed. We notice that for a network of Kuramoto oscillators, the only effect of increasing the dimension of the network is to slow down synchronization. On the contrary, we can observe a different phenomenon in networks of Rössler systems, where synchronization is not always attained.

Finally, we observe that a variation of the constant gains μ and α causes different consequences in the network of Kuramoto compared with the Rössler one. As we can see, for example, in Table 3, if we consider a network of Kuramoto, increasing μ, the convergence to the synchronous state is faster. In a network of Rössler, on the contrary, beyond a given threshold, the adaptive strategies are no more able to synchronize the network. Therefore, in practice, it is essential to carefully select the gains μ and α. Indeed, we can notice from Table 3 that an inconvenient choice of these parameters can lead to an asynchronous evolution of the network.

Table 1. Analysis of the performances of the different strategies.

	Kuramoto model					
	Vertex-based			Edge-based		
	Scale-free	Small-world	Random	Scale-free	Small-world	Random
t_s	22.4	20.0	22.4	29.57	36.66	31.13
σ_{min}	0.08	0.10	0.08	0.019	0.011	0.016
σ_{max}	0.70	0.71	0.73	0.43	0.44	0.46
Mean(σ)	0.37	0.38	0.37	0.16	0.16	0.16
Std(σ)	0.15	0.14	0.14	0.086	0.083	0.084
	Rossler system — coupling on x					
t_s	64.9	78.0	72.6	S.N.R	70.65	66.7
σ_{min}	0.04	0.05	0.04	S.N.R	0.034	0.032
σ_{max}	0.28	0.28	0.31	S.N.R	0.32	0.35
Mean(σ)	0.16	0.14	0.14	S.N.R	0.15	0.15
Std(σ)	0.047	0.035	0.044	S.N.R	0.053	0.055
	Rossler system — coupling on x, y, and z					
t_s	47.1	57.2	48.3	41.0	52.8	46.0
σ_{min}	0.21	0.37	0.037	0.017	0.019	0.016
σ_{max}	0.19	0.16	0.19	0.22	0.22	0.24
Mean(σ)	0.11	0.09	0.09	0.11	0.10	0.10
Std(σ)	0.035	0.023	0.027	0.039	0.035	0.037

Note: S.N.R, Synchronization not reached.

Table 2. Influence of the size of the network on synchronizability and convergence speed.

	Kuramoto model (vertex-based strategy, $\mu = 0.1$)	Rossler coupled x (edge-based strategy, $\alpha = 0.1$)
N (size of the network)	t_s (settling time)	t_s (settling time)
10	7.2	25.0
20	12.1	38.4
30	15.9	40.8
40	17.8	50.8
50	19.2	55.7
60	20.4	69.0
70	21.5	S.N.R.
80	22.0	S.N.R.
90	22.3	S.N.R.
100	22.4	S.N.R.

Note: S.N.R, Synchronization not reached.

Table 3. Influence of the gains μ and α on synchronizability and convergence speed.

	Kuramoto model (vertex-based strategy, $N = 100$)	Rossler coupled x (edge-based strategy, $N = 100$)
μ (α for the edge-based)	t_s (settling time)	t_s (settling time)
0.001	222	290
0.01	53.4	171
0.02	48.3	226
0.05	37.8	S.N.R.
0.1	22.4	S.N.R.
0.5	12.0	S.N.R.
1	5.2	S.N.R.

Note: S.N.R, synchronization not reached.

7. Adaptive synchronization of a network of non-identical oscillators

As a final test of the limitations of the adaptive strategies presented in this paper, we present the case of networks of non-identical Kuramoto oscillators. It is known that such non-identical oscillators would naturally oscillate at different frequencies and cannot, therefore, achieve complete synchronization. We observed that larger coupling strengths cause the oscillators to have closer frequencies. Namely, the control action provided by the adaptive synchronization strategies clusters effectively the phases, but does not guarantee a complete synchronization as shown in Figure 36, where a standard vertex-based strategy is used. This causes the coupling strengths σ_i to increase indefinitely, as shown in Figure 37.

To solve this problem, we propose an hybrid modification of the adaptive strategy presented in this paper. Specifically, we consider a saturation of the coupling gains so that when the time derivative of σ_i becomes lower than a fixed threshold, say $\hat{\sigma}_i$, it is automatically set to 0. In our simulations, we set this threshold equal to 0.2. Preliminary results shown in Figures 38 and 39 seem to indicate the viability of such an approach.

8. Conclusions

We have shown that synchronization can be successfully achieved by considering a set of novel adaptive synchronization strategies based on the local interaction between neighbouring nodes

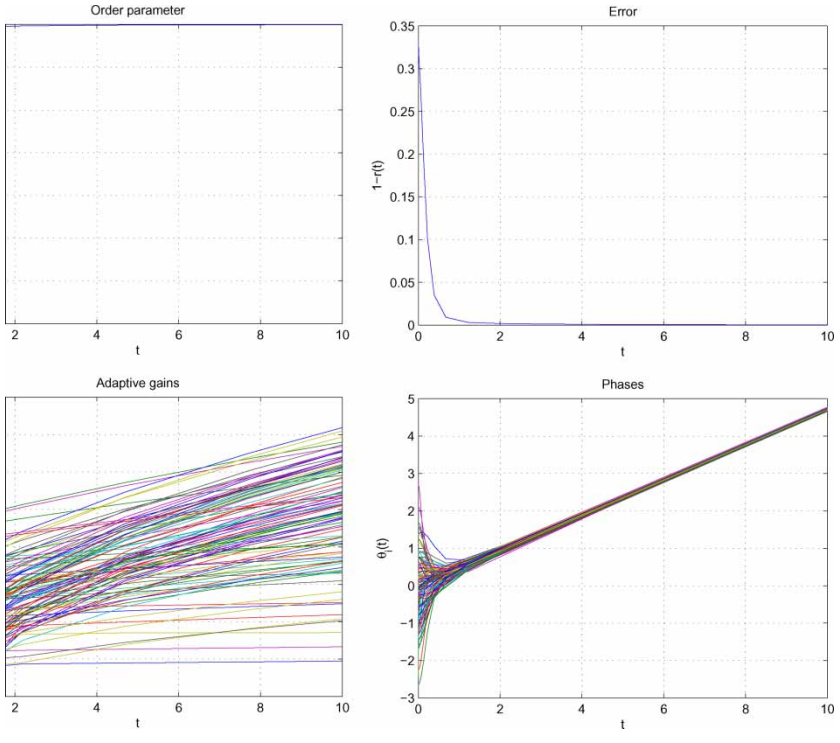

Figure 36. Evolution of order parameter (top left-hand panel), error (top right-hand panel), σ (bottom left-hand panel), and phases (bottom right-hand panel) in a BA network of Kuramoto using the vertex-based strategy choosing random initial frequencies.

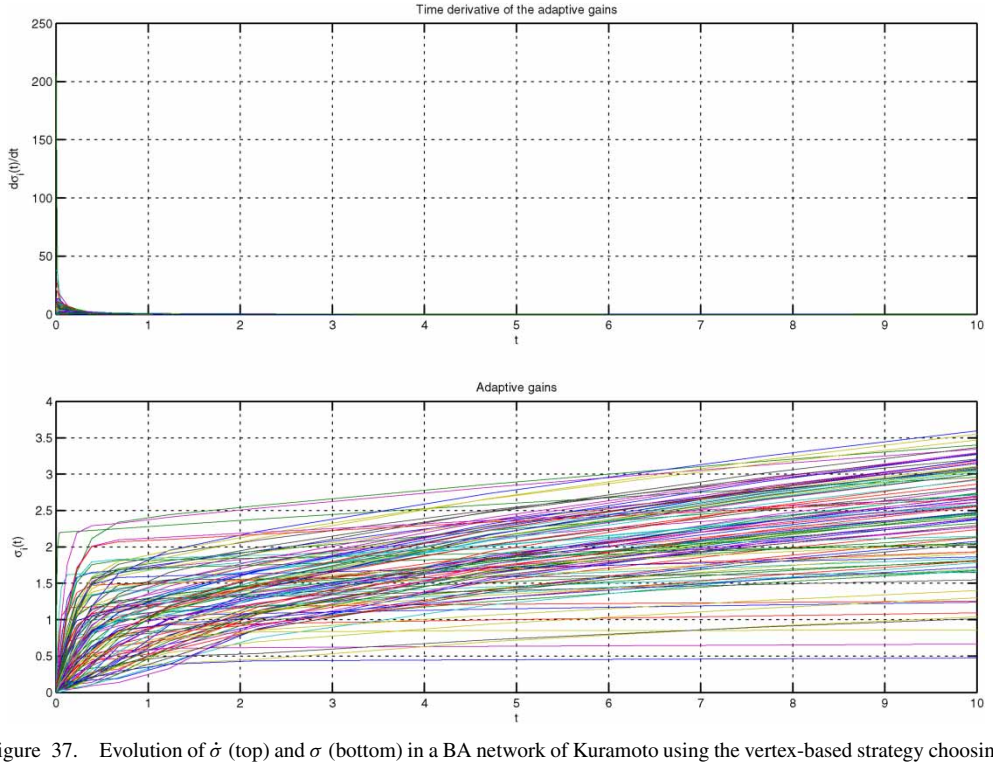

Figure 37. Evolution of $\dot{\sigma}$ (top) and σ (bottom) in a BA network of Kuramoto using the vertex-based strategy choosing random initial frequencies.

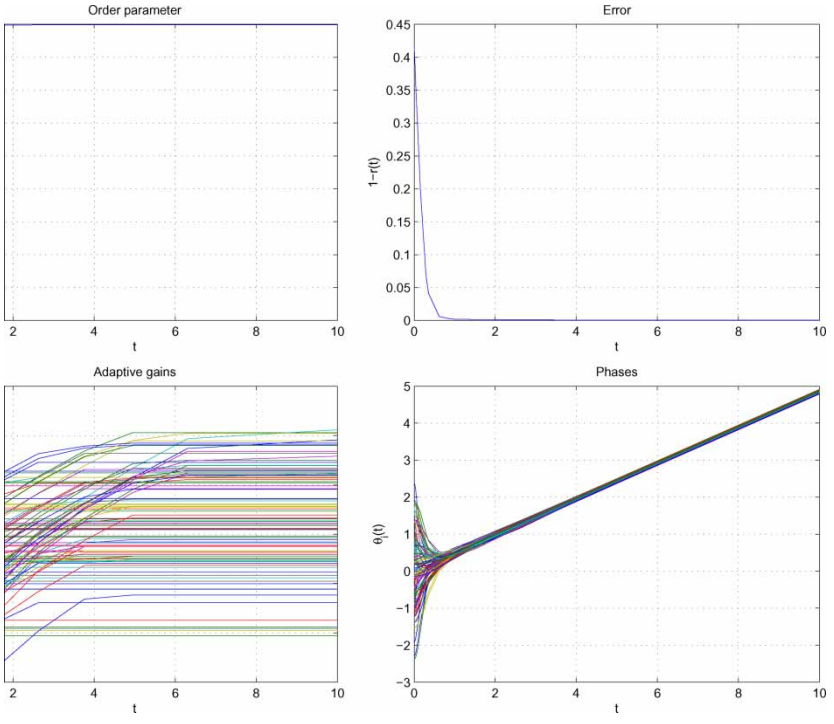

Figure 38. Evolution of order parameter (top left-hand panel), error (top right-hand panel), σ (bottom of the left-side), and phases (bottom right-hand panel) in a BA network of Kuramoto using the vertex-based switched strategy choosing random initial frequencies.

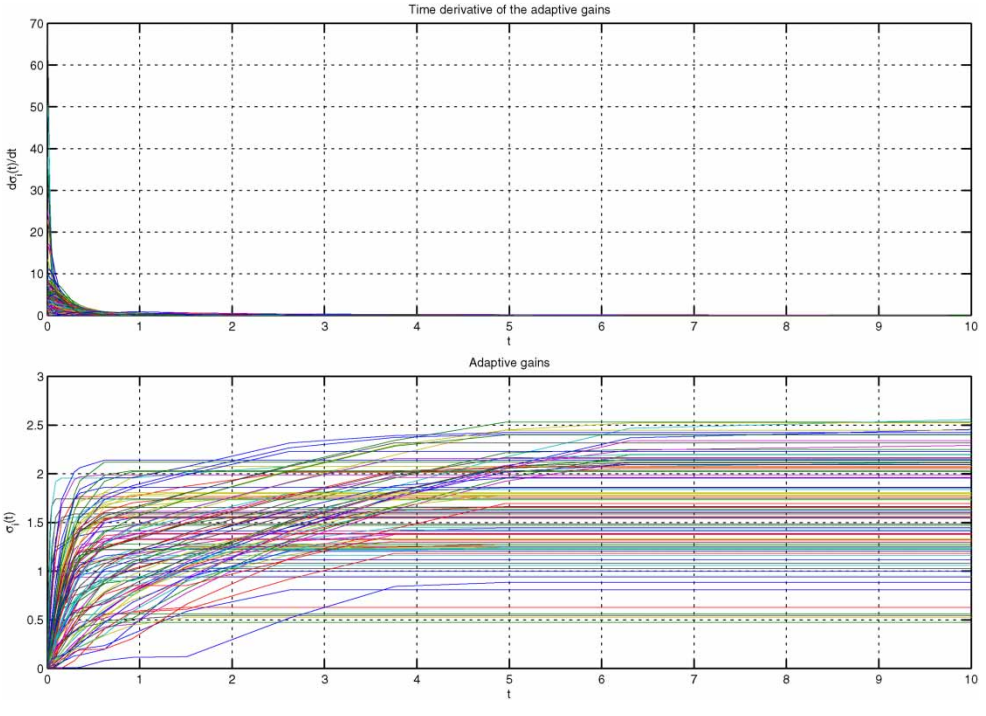

Figure 39. Evolution of $\dot{\sigma}$ (top) and σ (bottom) in a BA network of Kuramoto using the vertex-based switched strategy choosing random initial frequencies.

in the networks of coupled oscillators. Specifically, we proposed two alternative decentralized schemes for adaptive synchronization: vertex-based and edge-based. We validated both the strategies on a variety of different network topologies characterized by different node dynamics, showing the effectiveness of the adaptive approach on a number of different scenarios and its limitations. Current research is addressing the urgent open problem of proving asymptotic stability of the proposed synchronization scheme. Preliminary results in this direction seem to indicate that the asymptotic stability can indeed be proved by means of appropriate Lyapunov-based arguments. This is the subject of ongoing work.

References

[1] S. Boccaletti *et al.*, *Complex networks: structure and dynamics*, Phys. Rep. 424 (2006), pp. 175–308.
[2] G. Chen and Z. Li, *Robust adaptive synchronization of uncertain dynamical networks*, Phys. Lett. A 324 (2004), pp. 166–178.
[3] J.H. Fewell, *Social insect networks*, Science 301 (2003), pp. 1867–1870.
[4] R.A. Horn, *The Hadamard product*, Proc. Symp. Appl. Math. 40 (1990), pp. 87–179.
[5] Y. Kuramoto, *Chemical Oscillations, Waves and Turbulence*, Springer-Verlag, 1984.
[6] J. Kurths and C. Zhou, *Dynamical weights and enhanced synchronization in adaptive complex networks*, Phys. Rev. Lett. 96 (2006), p. 164102.
[7] J.A. Lu, J. Lü, and J. Zhou, *Adaptive synchronization of an uncertain complex dynamical network*, IEEE Trans. Automat. Control 51(4) (2006), pp. 652–656.
[8] C.C. Moallemi and B. Van Roy, *Distributed optimization in adaptive networks*, in *Advances in Neural Information Systems 16*, S. Thrun, L.K. Saul and B. Schölkopf, eds., MIT Press, Cambridge, MA, 2004, pp. 887–894.
[9] M.E.J. Newman, A.L. Barabàsi, and D.J. Watts, *The Structure and Dynamics of Complex Networks*, Princeton University Press, 2006.
[10] W. Ren, R.W. Beard, and E.M. Atkins, *Information consensus in multivehicle cooperative control*, IEEE Control Syst. Mag. 27 (2007), pp. 71–82.
[11] O.E. Rössler, *An equation for continuous chaos*, Phys. Lett. A 57 (1976), pp. 397–398.
[12] K.O. Stanley, B.D. Bryant, and R. Mikkulainen, *Evolving adaptive neural networks with and without adaptive synapses*, Proceedings of the 2003 IEEE Congress on Evolutionary Computation, 2003.
[13] X.F. Wang and G. Chen, *Complex networks: small-world, scale-free and beyond*, IEEE Circuits Syst. Mag. 3(1) (2003), pp. 6–20.